UNIVERSITY „ POLITEHNICA" OF BUCHAREST

DOCTORAL SCHOOL. APPLIED SCIENCES

Decision nr..... from.....

DOCTORAL THESIS RESUME

Development of techniques for ion-beam analysis and ion manipulation

Autor: Rotaru Ionuț Adrian

Supervisor : Prof. Univ. Dr. Gheorghe CĂTA-DANIL

DOCTORAT COMMISSION

Chairman	Prof. Dr. Daniela BUZATU	from	UPB
Doctoral supervisor	Prof. Dr. Gheorghe CĂTA-DANIL	from	UPB
Reviewer	CS1 Dr. Dimiter BALABANSKI	from	IFIN-HH
Reviewer	Prof. Dr. Mircea Iacob GIURGIU	from	UTCB
Reviewer	Prof. Univ. Emil PETRESCU	from	UPB

BUCHAREST 2020

Contents

Introduction

Ion beam technology is a field of techniques used for the creation of different types of charged particles, manipulating them through electric and magnetic fields and analysing them to investigate the properties of matter.

The full range of research topics, both basic and applied are vast and cannot be covered in any single work. However, the basic principles for all these applications shares a few simple processes. Namely, the understanding of the interaction of charged particles with electro-magnetic fields through the Lorentz Force, the processes of ion ionization that enables the creation of such ion beams and the principles of charged particles detection.

This thesis will present some of my work in the field of experimental physics and is centred around three experimental facilities. The work starts at the 3 MV Tandetron Accelerator at IFIN-HH where I was involved in multiple developmental programs. One such developmental work, albeit simple and not at all challenging proved to have the most significant impact as far as beam demand is concerned, so I choose to cover this topic in the first part. In the second part, the developmental work towards a system upgrade at the FRS at GSI will be covered. This is a facility that produces radioactive ion beams for mass analysis using the fragmentation method and the developmental work that was made, together with my colleagues, should enable a new production method that holds some promising research opportunities. In this thesis I will be covering my contributions towards this project. Finally, as I shifted my work towards ELI-NP and got engaged in the upcoming ELISOL experiment, that will provide radio-active ion beams through photo fission interactions, I will present my progress thus far towards the development of a smaller experimental system that could be used for testing purposes before work starts on the larger experiment. RF Carpets are relatively new devices used for the capturing and extraction of ion beams and my investigations into using such devices for the ELISOL experiment is presented. During this study, a novel RF carpet concept was developed that offers promising prospects. Finally, my work towards designing a testing unit for RF carpets is presented in the last part.

Experimental physics handles the design of new experimental systems, construction and testing. The main skills employed for such work are mechanical design and execution, design of electrical and electronics systems, ion-optics simulations and vacuum design. It is through these skills that I will be presenting my work in the following pages.

Chapter 1: Technology of accelerated ion beams and ion manipulation

1.1.Context

Accelerated ion beams are widely used for a variety of applications, both in research and in industry. In research we can distinguish two major categories: basic physics and applied physics. The most common industrial application is ion implantation with dopants.

There are many other applications of accelerated ion beams. Generally, these applications use accelerated beams at keV and MeV energies (for example 3 MeV for IBA, 1 MeV for ^{14}C dating, etc.). Some of these applications include ion beam milling, ion beam imaging etc.

If in fundamental research the tendency was towards the realization of ever more increase in energies using large acceleration, in applied research the trend has been to increase the accuracy of measurements by using precision instruments.

1.2.Basic principles of a particle accelerator

In its simplest form, a particle accelerator system must do three things. First, it must form an ion beam (molecular ions, atomic ions, fundamental particles, or nuclei) using an ion source. The most important properties of such a beam are purity (for an ion beam, the beam must be mostly composed of the ion species we are interested in), beam energy, particle flux (usually measured in beam current) and the shape of the beam (its diameter, cross section etc).

Second, the system must accelerate this beam to the required energy with a reasonable efficiency. The usual energies for small accelerators are from keV to a few MeV. Larger synchrotron accelerators used for heavy ion collision experiments can accelerate up to GeV and beyond. The acceleration system must provide a good energy resolution expressed dE/E (which is an indication of energy spread) which is usually less than 1E-2 for small research accelerators (for example at an energy of 1 MeV resolution is +/- 10 keV for a Tandetron accelerator). Thus, the most important properties of this system is the obtained accelerated energy, energy resolution and transmission factor (the ratio between accelerated beam current and injected beam current).

Third, the accelerated beam must be directed towards a reaction chamber (where the accelerated projectiles will interact with a stationary target) and this process involves guiding the beam using various electro-optical systems and beam diagnostics to meet the conditions required for the experimental needs. The expression "carry the beam on the target" is popularly used to describe the process by which the beam is directed from the ion source into the accelerator system, through electro-optical manipulation instruments and correction systems and up to the target where the reactions takes place.

1.3.Ion sources

The ion source has the role of forming the ion beam from either a gas or a solid extraction compound. Over the years several techniques have been developed for obtaining ion beams and for each technique there are several variants of ion sources. Based on their physical principle of operation, these techniques can be divided into three main categories: ion sources with electron or ion bombardment, radio frequency ion sources and voltage breakdown ion sources.

1.3.1. Cesium sputtering ion source

The cesium sputtering ion source is an assembly of two ion sources: one is a thermal evaporation ion source and the other an ion bombardment ion source. This is mainly used to obtain negative ions from a solid extraction compound. A cesium reservoir is heated to approximately 80-100^{0}C under low pressure and the cesium will evaporate and diffuse through the ionization chamber, condensing on its walls. Inside the ionization chamber, a heated plate of around 1000^{o}C is used as an ionizer. When cesium vapors enter in contact with this heated plate, it will form positive cesium ions that will be accelerated towards the cathode that contains the extraction compound. This cathode is negatively charged by comparison with the ionizer plate, which is positively charged by comparison. Under the cesium bombardment, the extraction compound will sputter fragments (mostly compound molecules and atoms). Fig. 1 illustrates the basic working principle of this type of ion source.

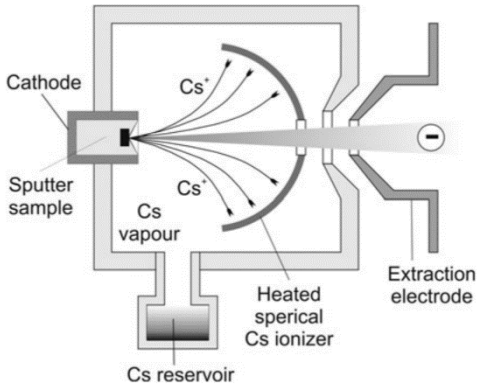

Figure 1: Illustration of a cesium sputtering ion source

To optimize the efficiency of a cesium sputtering type ion source used at the 1 MV Tandetron accelerator at IFIN-HH, the entire accelerator system, together with the ion source were modeled in 3D and ion optics simulations were performed. This was useful to deduce optimal working parameters and to further improve the system by studying new geometries. A simulated cesium ion source is presented in Fig. 2.

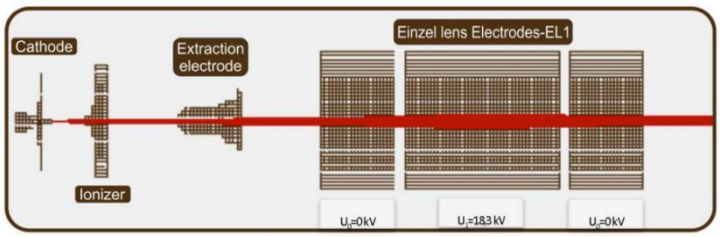

Figure 2: 2D simulation of the cesium sputtering ion source and the first electrostatic Einzel lens used for beam containment

1.4.Electrostatic accelerating systems

After the ion beam is formed, it is injected into an accelerating system that has the role of increasing the kinetic energy of this beam until it reaches experimental needs. In theory, the simplest type of electrostatic accelerator consists of two metallic plates on which a voltage drop is applied. These parallel plates need to have an orifice in the center such that, through one plate an ion beam can be injected and through the other, the ion beam can be extracted. In practice, such system is complicated to engineer.

To ensure constant acceleration throughout the acceleration system, the electro-static field must be maintained as stable as possible. For this reason, an accelerator system uses many metallic electrodes connected through a resistor chain. The voltage drop is applied between the end electrodes and the inner electrodes become intermediary electrodes. Equipotential must be formed between each pair of two electrodes. By using this technique, field fluctuations are minimized, and kinetic energy gain becomes predictable. The most important parameter in this type of accelerator is energy resolution which is directly proportional to field fluctuations. A simple acceleration structure is presented in Fig. 3.

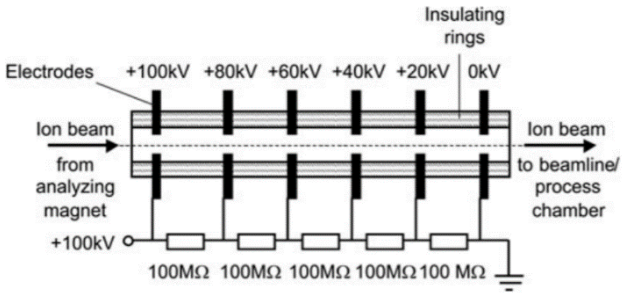

Figure 3: Illustration of a concept acceleration system with a voltage divider chain

1.5.Ion beam handling

After an ion beam is generated by an ion source and accelerated through an accelerator structure, it can be directed towards a reaction chamber and be used for the various experimental needs. For example, it can be used to form a reaction, or it can be directed towards a detector for analysis (in the case of accelerated mass spectrometry applications). To ensure the quality of the ion beam, it must be at several points monitored and filtered.

Important properties of an ion beam are the energy, beam current, purity, and geometry. The kinetic energy is adjusted using the accelerator voltage and the resolution depends on the stability of the high voltage generator. Beam current is controlled from the ion source and is limited to the maximum current the high voltage generator can supply without compromising stability.

The purity of the beam cannot be controlled from the ion source. Through beam purity, we understand the ratio between the number of ions from the species of interest to all other ions, including molecular ions. For example, in using the cesium sputtering ion source, if we want to obtain a hydrogen beam, we can use TiH_2 as an extraction compound. By doing this, we would obtain a hydrogen beam mixed with titanium ions and other trace elements, such as

copper, iron, oxygen etc. In principle, the purity of the beam should be as high as reasonably possible and values greater than 99% are desired.

Finally, the beam must interact with the target so it must be deflected both horizontal and vertical to gain control of beam alignment. The interaction area can be adjusted by focusing the beam with electro-optical lenses, from beam sport of tens of cm^2 up to a few um^2. Finally, the beam profile must be corrected. All these adjustments need to be performed until the beam meets the requirements for the experiment.

Based on the results discussed in Sub-chapter 1.3.1. an article was submitted to Romanian Reports in Physics.

Conclusions

This chapter has introduced the basic concepts of ion manipulation that will be explored throughout this thesis. The ion beam simulation presented in sub-chapter 1.3.2. was part of a larger effort to model the entire 1 MV Tandetron accelerator at IFIN-HH and the results produced several articles and a PhD thesis. Because of my participation in these simulations, a paper was submitted with myself being the corresponding author. I would like to thank my colleague Doru Pacesila for a fruitful collaboration while working on the simulations together.

In Chapter 2, the workings of the 3MV Cockcroft-Walton type Tandem accelerator at IFIN-HH will be further explored. This accelerator was upgraded with a system to allow extraction of the ion beam into air to provide in-air IBA and my contributions towards the realization of this system is presented.

Chapter 3 presents the experimental progress towards designing and building of a target wheel system to allow production of radioactive ion beams using the method of multi-nucleon transfer at FRS, GSI.

In Chapter 4, the methods of ion trapping are further explored and my contributions towards the design of such a trap to be used to produce radioactive ion beams are presented.

Chapter 5 presents the design work of two experimental systems used as a prototype for testing of RF Carpets as ion traps and to serve as a technological demonstrator towards the realization of the ELISOL experiment, a large experimental facility planned to produce and study radioactive ion beams at ELI-NP.

Chapter 2: External ion beam

2.1. Context

External ion beams are obtained through extraction of accelerated ions into the air through a thin window that must affect the beam as little as possible. Such external ion beams have many advantages; they provide non-destructive and non-invasive analysis and target samples are easier to analyse at atmospheric pressure than in vacuum. Because of this, many laboratories worldwide developed dedicated external ion beams to be used for ion beam analysis.

Sophisticated ion beam analysis techniques have been developed in recent times to be used with external ion beams, techniques that were traditionally reserved for in-vacuum measurements only. Some of the most important used today are particle induced X-ray emission [1], in-air ion backscattering [2], elastic recoil detection analysis [3], scanning transmission ion microscopy [4] and ion beam induced charge. These techniques are illustrated in Fig. 4.

Despite the competition with other facilities (synchrotron light sources, nuclear reactors, electron microscopes, x-ray fluorescence) ion beam analysis techniques remain very competitive because of its ability to provide multiple types of complementary measurements simultaneously (x ray induced emissions for light atoms, elastic recoil detection for hydrogen profiling, backscattering for depth profiling). These techniques are applied simultaneously and can be configured according to the experimental needs of the specific target sample.

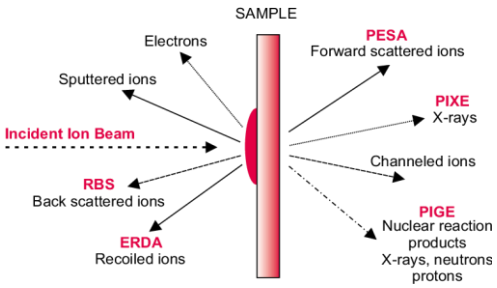

Figure 4: Ion beam analysis methods

2.2. Material analysis at the 3 MV Tandetron Accelerator at IFIN-HH

The experimental infrastructure at IFIN-HH was consolidated in the year 2012 with the commissioning of three new accelerators, alongside the existing 9MV Tandem, namely two Tandetron accelerators and one cyclotron for medical isotope production. The two Tandetron accelerators are electrostatic machines with Cockcroft-Walton high voltage generators and particularly good beam stability, making them very efficient for applied sciences. One of these is a 1 MV machine used for radioisotope dating and the second is a 3 MV Tandetron specifically designed for ion beam analysis [5], e.g. material analysis, material irradiation, implantation, and cross section measurements. The technical schematic for this machine is presented in Figure 5.

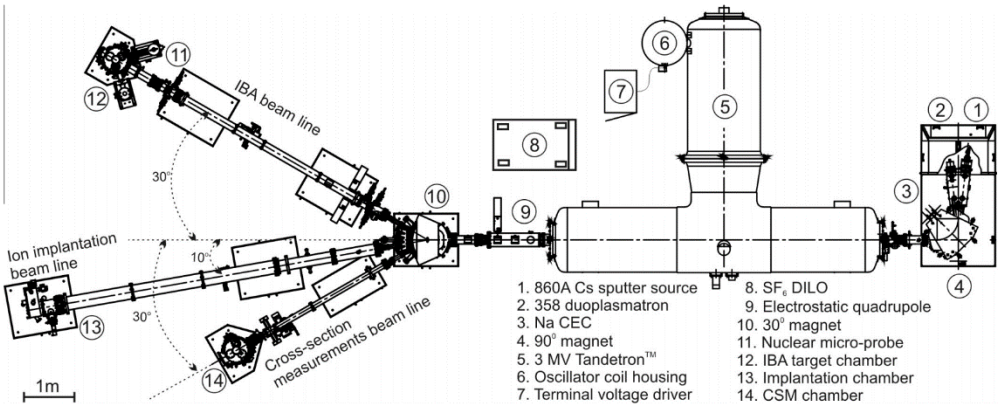

Figure 5: Technical schematic of the 3 MV Tandetron at IFIN-HH

Presently, the 3 MV Tandetron accelerator is used in a large variety of PIXE (particle induced X-ray emission) experiments. In these experiments, large arrays of samples are analysed from various fields of research, such as medicine and pharmacology, archaeometry, ecology and material engineering. This method of analysis provides several important advantages, such as:

- *High sensitivity*: in routine experiments, detection limits are around 0.1 – 1 ppm; they can vary according to the nature of each individual sample;
- *Versatility and the possibility for direct analysis*: with the current set-up, almost any solid object can be irradiated for PIXE experiments; for the analysis of heavier and larger objects, the ion beam needs to be extracted outside the reaction chamber for proper analysis.
- *Possibility of analysing liquid targets*: By using the experimental device designs for in vacuum analysis of liquid residue applied to a thin mylar foil; multiple targets can be prepared and analysed sequentially using the target wheel; this was the first technical upgrade for this accelerator that used in part 3D printing components and is illustrated in Fig. 6;

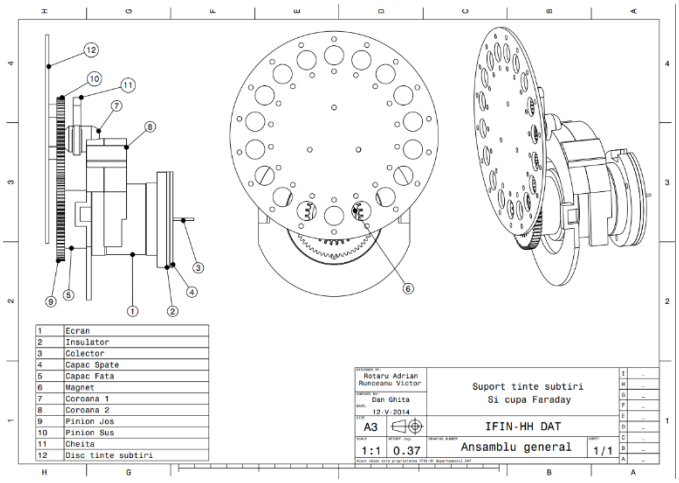

Figure 6: Target wheel developed for the analysis of liquid residues

- *Good spatial resolution*: the ion beam can be focused into a narrow beam, thus allowing positioning the beam with high precision;

- *Non-destructive analysis*: the technique allowed the analysis of delicate objects, targets that are organic in nature or very fragile without risking destroying them;
- *Multi elemental analysis*: Using the PIXE technique together with the 3 MV Tandetron accelerator, we can identify chemical elements between Z=13 (Aluminium) and Z=92 (Uranium).

2.3. Physics considerations of particle induced X-ray emission analysis at IFIN-HH

Characteristic X-ray emissions are a result of high energy ion-atomic interactions from the target surface between the high energetic incident ions (1 – 3 MeV) and target atoms. This incident ion beam can create atomic excitations or can eject electrons from their inner atomic shells. When this happens, a vacancy is left and an electron that occupies a higher energy state will occupy this vacancy. During this de-excitation atoms with emit photons with energies between 1 and 30 keV. Because every atom has a unique electron configuration, a material can be chemically analysed using the yield and the energy of emitted photons. By using the micro-focused beam, atomic distributions can be mapped throughout the surface of the material. This process is summarized in the diagram shown in Fig. 7.

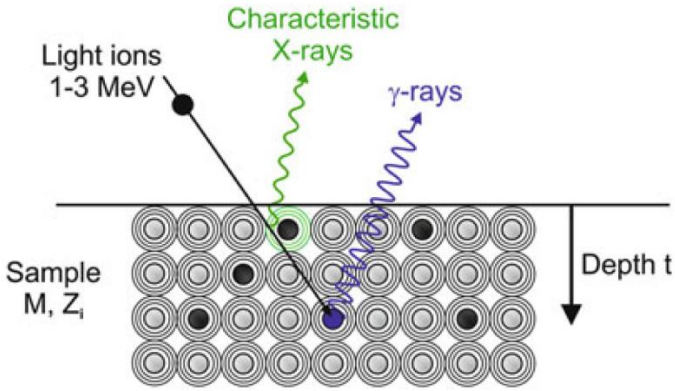

Figure 7: Physical schematic of ion induced photon emission from atomic electron shells

2.5. Fine tuning the nuclear microprobe electrostatic quadrupole

The electrostatic quadrupole, located before the entrance to the IBA chamber, can be used to precisely focus a micro beam inside the chamber target and this can improve measurement results significantly, at least in some cases.

While this system was designed for beam focusing inside the reaction chamber, it can be used to focus the beam right before it is extracted into air, such that the beam spot will be decreased, making it possible to perform in air micro-PIXE. To accomplish this, the entire quadrupole system was simulated using the SimIon 8.1 ion optics software [6]. The geometry was designed in a CAD software and was imported as .STP file.

At the entrance to the quadrupole, the simulated beam is collimated with an aperture of 2 mm in diameter. A beam profile monitor is placed on the extraction window and the beam normal distribution is calculated for every voltage potential applied. The distribution of the beam on the extraction windows is plotted in Fig. 8 for both X and Y components. The effects

of the quadrupole on the beam spot is clearly demonstrated, the focusing on the X plane is more pronounced than on the Y plane at smaller potentials, however when the potentials increases, these phenomena will invert. This happens because the X plane is the first to be focused.

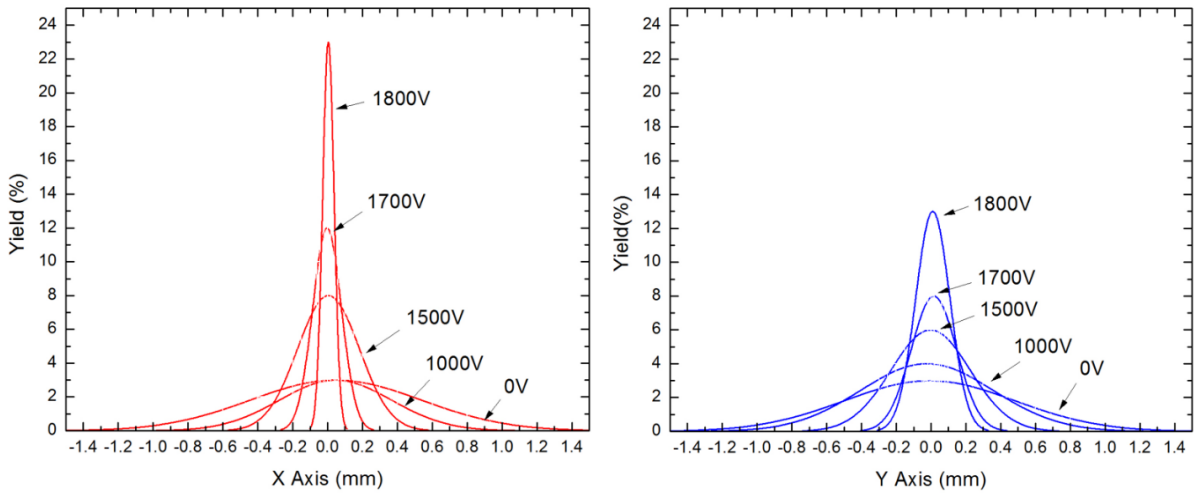

Figure 8: Lateral beam distribution on the extraction window for various voltage potentials

The contribution of the electrostatic quadrupole is clearly seen, and it can be used as an invaluable tool to probe into small areas, for example in small defects or cracks. From the normal distribution of each configuration, the FWHM for both X and Y components was calculated and are shown in Fig. 9, as well as the total beam area as a function of quadrupole voltage.

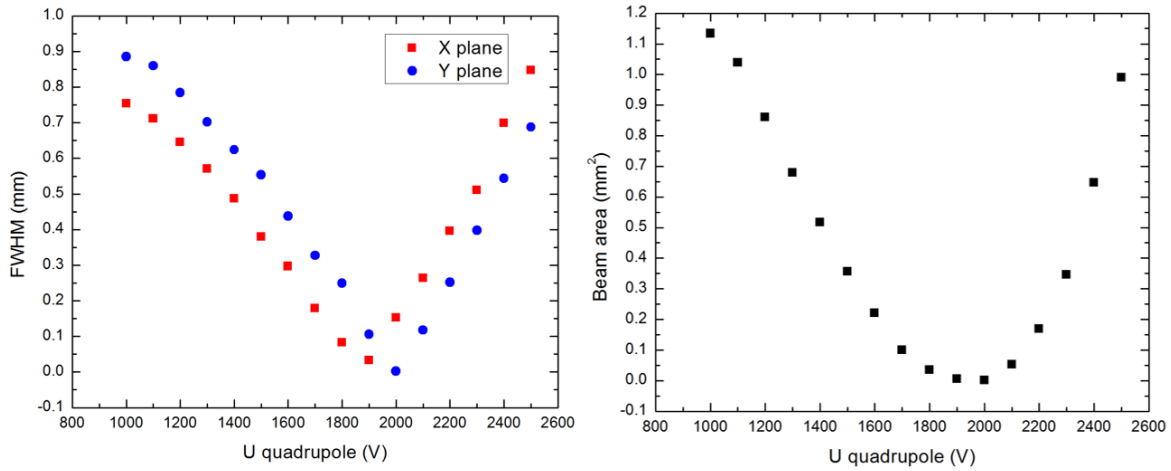

Figure 9: Simulated results for lateral beam profile; left: FWHM and beam area as a function of quadrupole voltage

Using this information, the potentials can be optimized to produce the smallest values of FWHM. Because the beam does not have the same profile in both X and Y directions, three specific cases are defined that can be used for various applications. Firstly, we can optimize the beam in the X direction for minimum FWHM that will produce a narrow line, secondly this can be done for the Y direction and thirdly we can optimize for overall circular beam area which will be a compromise. These values have been calculated below:

Optimal potentials for electrostatic quadrupole for different beam parameters

	U	FWHM X	FWHM Y	Beam area
Minimum X profile	1872 V	1.8 µm	158 µm	483 μm^2
Minimum Y profile	1999 V	148 µm	2.3 µm	578 μm^2
Circular profile	1935V	73 µm	73 µm	0.01 mm^2

2.6. Design and construction of the beam extraction setup at IFIN-HH

An ion beam can only be extracted into the air using a beam extraction window. This is constructed from a special material that needs to be strong enough to resist the forces created by the pressure difference acting on its sides, which are significant. As an example, the IBA reaction chamber is kept at a low pressure of around 10^{-6} mbar and the outside ambient pressure is around 1.013 bar, resulting in a net force of around 10 kg/cm^2 or $100g/mm^2$. Because of this, the extraction area needs to be small at around a few square mm. Secondly, the extraction windows need to affect the beam as little as possible. While the beam passes through the window it will experience stopping power and the beam will straggle, so the extraction windows also needs to be very thin.

To monitor beam current, we can use an external Faraday cup. By taking measurements before sample irradiation and assuming current stability total charge can be integrated and as such the ion current that irradiates the sample can be calculated. Another system configuration is to place an X-Ray detector to watch for characteristic X-ray emitted by the window to indirectly measure the current. A Faraday cup is necessary to correlate between beam current and characteristic X-ray counting rate.

This method has the advantage of continuous and accurate measurements. For these we have chosen a Si-PIN detector from Ametek, model X-123 [7] with resolution of about 145 eV at 6 keV, which is sufficiently for our needs. The detector is very compact, comes in a small form-factor and has included all needed electronics. The detector comes with LabView support and was incorporated in our control environment.

The detector was positioned at 45^o with respect to direction of the incident beam and the tip must be placed in vacuum. A mechanical frame to house the detector is attached to the Si3N4 window by using a special vacuum glue. The CAD design and the finished assembly is shown in Fig. 10. It contains connection for the 0^o IBA chamber access port, where it will be mounted, a vacuum valve to close the extraction for maintenances and when not in use to limit the possibility of an accidental window break, a mechanical holder for the extraction windows itself and a port specifically designed for the SI-PIN detector. Everything is made from non-magnetic stainless steel.

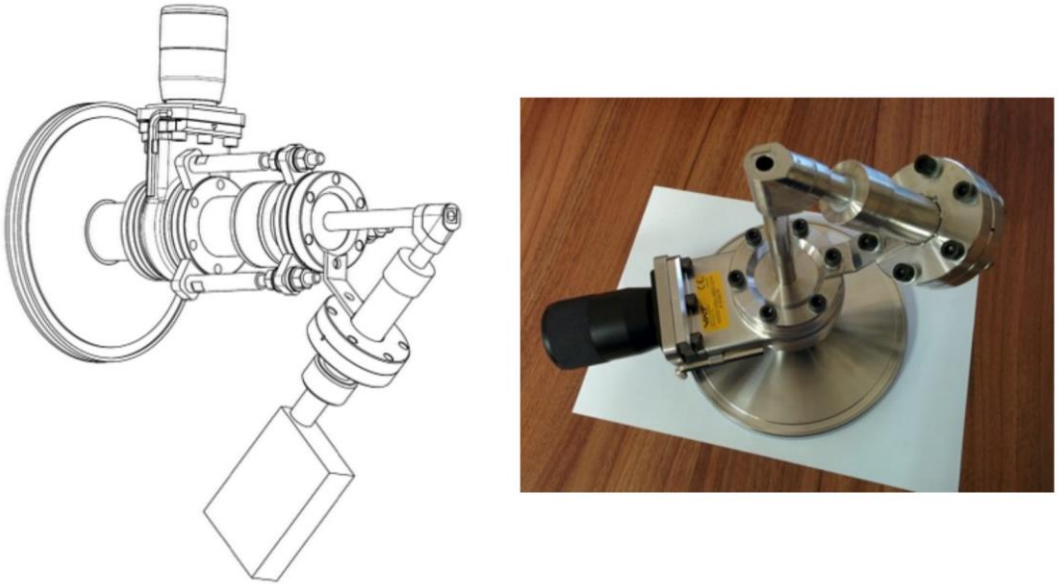

Figure 10: Beam extraction setup; left: CAD model, right: constructed assembly

2.7. External ion beam testing

To evaluate the quality of the extracted beam we have performed a batch of different tests. First, a radio chromic film was placed in air, at the exit of the extraction window and was irradiated using protons of 3 MeV energy. This film is presented in Fig. 11. Radio chromic films are a type of self-developing films that are invaluable for testing and characterisation of various types of radiation generators and ion beam installations. The film changes colour when exposed to ionising radiation proportional to the amount of absorbed energy so the amount of exposure can be recorded easily. Also, they have overly sensitive spatial resolution and the geometrical profile of the beam is easily distinguishable. Furthermore, these films are insensitive to visible light and as such are quite easy to use. [8]

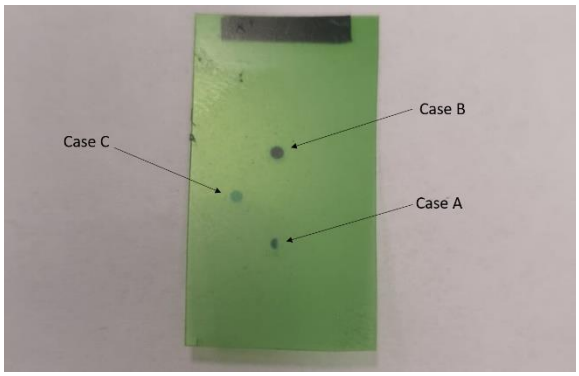

Figure 11: Radio chromic film with different exposures used to test external proton beam quality

To further analyze the beam distribution an electronic microscope camera was used. This allows us to plot the color intensity gradient and transform image exposure to absorbed radiation dose.

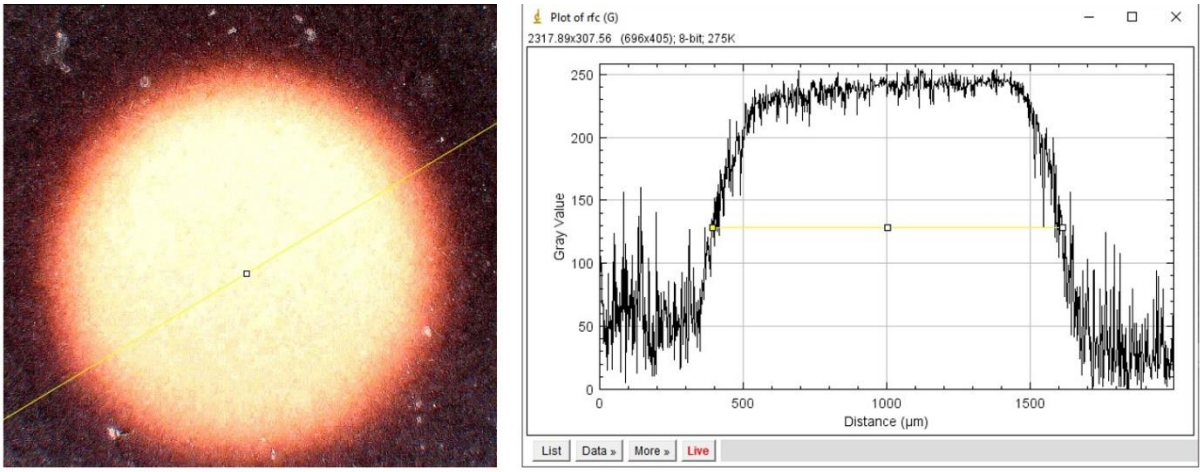

Figure 12: Electronic microscope analysis of defocused circular beam spot

Finally, the system was tested by performing an in-air PIXE measurement on a Standard Reference Material (SRM) [9]. This are certified wafers with diameters between 12 to 14 mm that contain certified mass fractions values and are useful for development of analysis methods for detecting trace elements. For this experiment, we have used the 611 SRM which contains certified values for 15 elements that can be cross referenced with our own measurement. This Standard Reference Materials are valid indefinitely and can be used for periodic testing of the quality of the system.

The following PIXE spectrum was obtained using 3 MeV proton beam with an exposure time of 5 minutes.

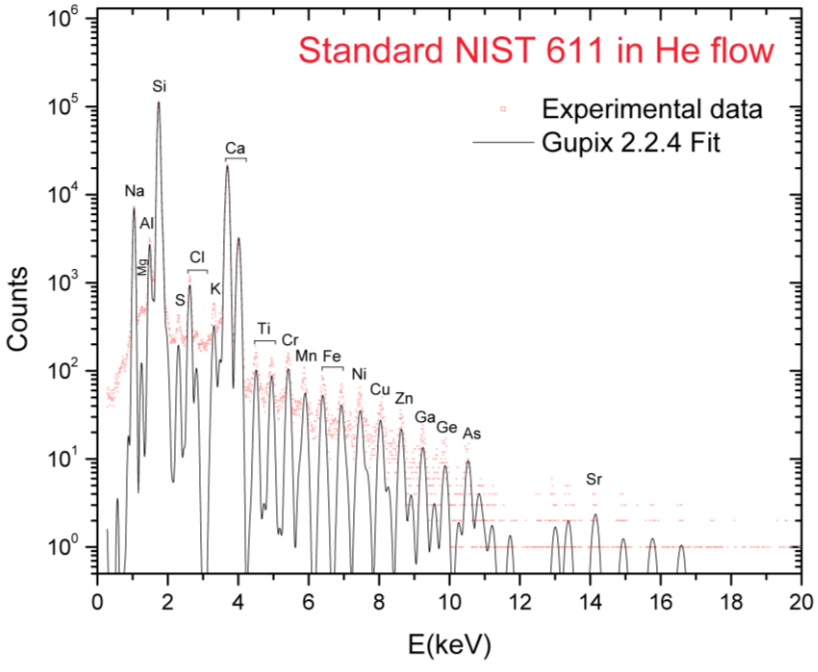

Figure 13: In-air PIXE measurement on SRM 611

Most of the chemical elements from the reference material are clearly seen in the spectrum as very distinguishable peeks. The spectrum was processed with Gupix software and most of the lines are easily resolved. Although in-air PIXE does not yields the same resolving

power as an in-vacuum measurements, the quality of the obtained spectra is particularly good and in perfect agreement with the provided reference mass fractions [9].

Based on the results discussed in this chapter, an article is in advanced preparation and is planned to be submitted to Romanian Reports in Physics.

Conclusions

A new experimental setup for in-air PIXE was developed at the 3 MV Tandetron accelerator, IFIN-HH. The entire system has been tested and it is functioning accordingly. Thus, the experimental infrastructure has been updated with a very practical technique that will be mostly geared towards investigations of objects of cultural heritage, but it will also be used for a variety of other applications.

The external beam has been tested using radio chronic films to visualize beam irradiation spot. Finally, an in-air PIXE analysis has been performed on a Standard Reference Material to validate that everything works properly. A long exposure photograph of a proton beam extracted in-air can be seen in Fig. 14. The blue glow of ionized nitrogen atoms shows the dispersive characteristic of the beam, as well as the total projected range. The picture has been color-corrected with increased luminance to make the beam more visible.

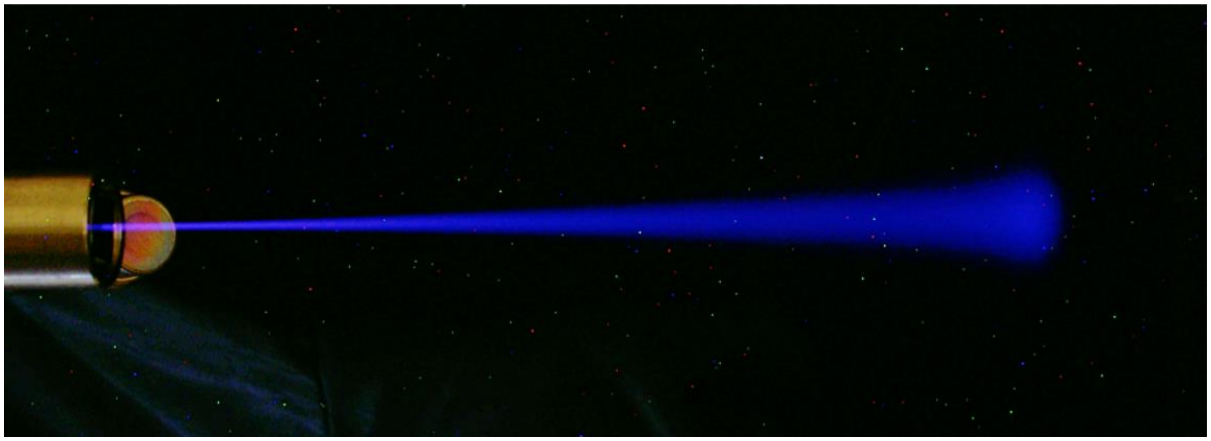

Figure 14: Long exposure picture of in-air proton beam

Chapter 3: Target Wheel

3.1. Context

Isotopes are created in stars while they evolve by changing their composition. They progressively burn through their hydrogen-shell, followed by the burning of the helium-shell, and continues to burn through higher elements. As it approaches its end, a star will go through different processes based on its original mass. Low-mass stars will eject their composition as stellar winds, and they will form planetary nebula while higher-mass stars will eject their composition more suddenly through an event called a supernova. This phenomenon is triggered by a gravitational collapse that is directed inwards and will produce sufficient pressure and temperature to trigger burning of carbon, oxygen and silicon. Heavier elements up to iron-56 are created during the compression shockwave caused by gravitational collapse that briefly increases temperature. This is the end of stellar nucleosynthesis and results in creating some of the most abundant isotopes in the universe in the range up to mass 56.

Isotopes heavier than 56 are mainly created by one of the three capture processes, slow neutron capture, fast neutron capture or proton capture. The various methods used to create the elements present today together with their relative abundances in which they are found is presented in Fig. 15.

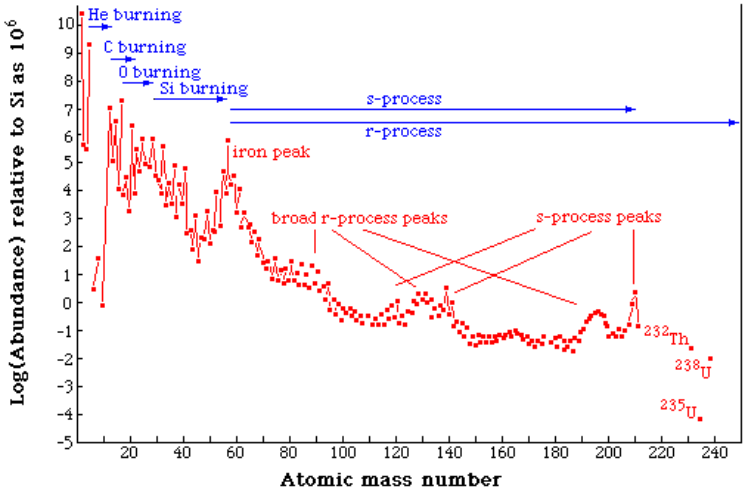

Figure 15: Distinct epochs of nuclear processes

Through the study of nuclear reactions and the rates by which they occur in cosmic like environment, nuclear astrophysics is a complex puzzle that tries to determine the origin of isotopes and describe the cosmic evolution of elemental abundances. In the last decades, study of neutron-rich isotopes that are close to the r-process path has become one of the main goals for modern radioactive isotope beam (RIBs) facilities worldwide. The study of exotic isotopes requires creating them in sufficient quantities in specialized laboratories and capturing them in traps. Two different approaches are used today for creating RIBs: Ion Source On-Line method (ISOL) and In-Flight method [10].

The ISOL method requires high current primary beam of light particles that are used to irradiate a thick hot target from which resulting isotopes will diffuse into an ion source, forming

an ion beam through secondary ionization. The method is slower compared to In-Flight approach but yields RIBs with particularly good optical quality since this depends only on the ion source.

The In-Flight method (also called the Fragmentation method) requires primary beam of heavy particles (for example uranium) that are used to irradiate a thin target, resulting in fragmentation of the primary beam. The resulting fragments are captured using a gas ion stopper and separated. This method produces on average smaller yields because of the inherent difficulty in accelerating high currents of heavy ions, however it is capable of faster extraction times when compared to ISOL methods. This is an important property to consider because radioactive isotopes are unstable and the more exotic they are, the shorter their life-time is. The FRS Fragment Separator at GSI, in Germany is a good example of the technique used for in-flight production of RIBs (Fig. 16) [11].

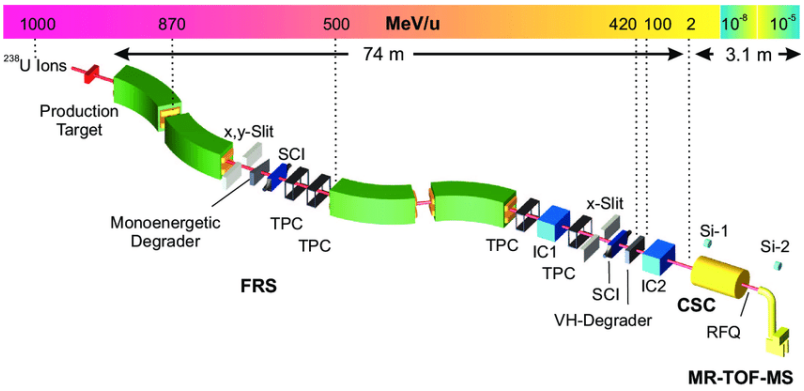

Figure 16: Experimental setup of the FRS Ion Catcher at GSI

Of current interest is the regions from the neutron-rich lanthanides to the neutron-rich actinides. Nucleosynthesis in these regions is thought to place through r-processes in cosmic locations such as neutron star mergers. Unfortunately, the methods typically used at this facility like fragmentation, fission or fusion cannot reach these areas and can only study reactions in the lighter region (A<160). Because of this, multi-nucleon transfer (MNT) reactions are considered to study these largely uncharted regions of heavy exotic nuclei.

Multi-nucleon transfer is a type of nuclear collision that take place between an accelerated projectile and a stationary target at energies slightly above the Coulomb barrier and at small impact parameters. It is a deep-inelastic collision in which several nucleons are transferred between projectile and target while they form a semi-bound system and, because of the conservation of momentum of the incoming projectile, the semi-bound system will rotate rapidly. Due to centrifugal forces, the semi-bound system will break apart and what emerges is a projectile-like fragment (PLF) and a target-like fragment (TLF). These are the initial projectiles and targets that exchanged nucleons and thus, through this process creation of new isotopes is possible. The method is however complex and is not completely understood, even though it has been studied for a few decades.

Compared to the other methods used at In-Flight RIBs facilities like fragmentation, MNT is observed to produce neutron-rich isotopes with an increased cross section of even some order of magnitudes, for example in the regions between ^{136}Xe and ^{198}Pt [12]. It is for this reason that there is an increased interest in experimenting with MNT type reactions to produce exotic nuclei towards the r-process path that might help in understanding of various nuclear

factors like shell energy levels or deformations. This might typically start by using both projectiles and targets that are as neutron rich as possible.

It has been proposed to establish and develop a new research direction at the FRS Ion Catcher for the studying of heavy neutron-rich isotopes through the multi nucleon reaction method. This will be done by using stable ^{238}U primary beam with energy of around 10MeV/u on neutron rich targets like ^{64}Ni, ^{209}Bi, ^{164}Dy, ^{198}Pt and it will be used to measure the production cross sections of both projectile like fragments and target like fragments simultaneously. This will also allow mass measurements of long-lived isomers (half-lives greater than a few ms) and their isomer-to-ground state ratios. Thus, new isomers can be discovered in MNT reactions.

3.2. Experimental design requirements

The FRS Ion Catcher is the main experiment used at GSI for catching and analyzing fragmentation products that are created using primary beam of ^{238}U accelerated through the SIS18 Synchrotron directed towards light targets. Once produced, fragments are cached using a gaseous chamber and extracted into a radioactive ion beam through a radio-frequency beam transport system and measured using a mass discriminator. It consists of three main sub-systems.

The cryogenic stopping cell (CSC) shown in Fig. 17 is a system of chambers filled with high purity helium that is cooled to 70K and continuously recirculated into the chamber. The inner chamber contains the helium gas and acts as a buffer for the fragments to be thermalized and directed towards an extraction nozzle with the use of guiding electric fields, both DC and RF. The outer chamber is used for insulation in order to keep the temperature of the inner part constant. Inside the stopping cell, an electrode structure provides a DC field for guiding thermalized ions towards the extraction side. Here, a radio frequency carpet [13] captures the fragments and guides them towards an extraction nozzle.

The RFQ beam line is composed of radio frequency quadrupoles, radio frequency switchyards and beam diagnostic instrumentation like Si detector, channeltron detector, Cs thermal ion source etc. This system also has a laser ablation ion source to allow production of calibration beams for the mass analyzer. This consists of a multi reflection time of flight mass spectrometer (MR-TOF-MS) that has a mass resolving power greater than 10^5 m/Δm. The entire FRS Ion Catcher, containing the CSC, the RFQ beamline and the MR-TOF-MS is presented in Fig. 17.

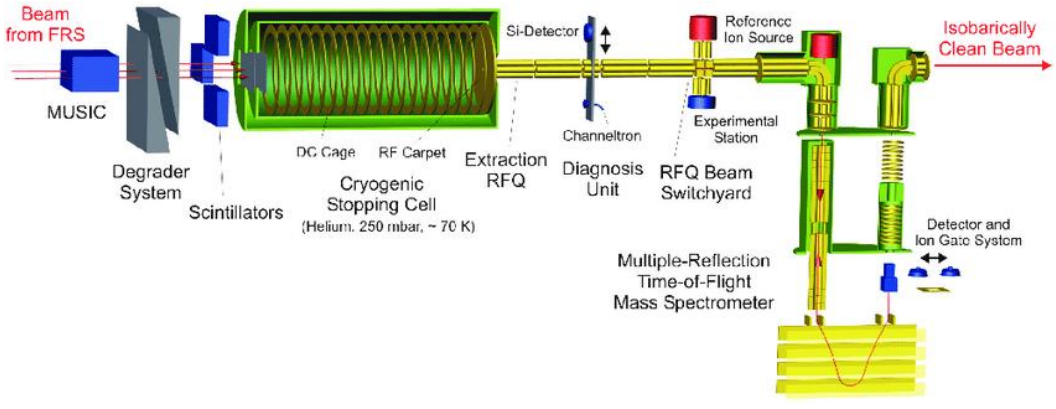

Figure 17: Schematic figure of the FRS Ion Catcher setup [11]

To study multi nucleon transfer reactions with the FRS Ion Catcher, a target system was needed inside the cryogenic stopping cell to enable MNT reactions.

The target system needs to fulfill several requirements. It requires a target wheel that can hold up to 6 thin targets and that can be changed sequentially, aligning each target, one at a time directly into the path of the primary beam. It requires a secondary target wheel that can accommodate either instrumentation like a beam dump for blocking incoming primary beam or Si detector for beam measurement, but it can also be used as a secondary target holder for thin targets. It requires a detachable holder for an ion source such that some experiments can be performed without using accelerated primary beam but relies on the internal ion source. It requires two collimated apertures placed at different angles to collimate the wide emission angle of the ion source. Lastly it requires an internal chamber that is properly shielded such that, when the ion source is mounted, ions will only escape through the collimated aperture.

This target system was designed at ELI-NP, Romania [14] and was manufactured at SOREQ, Israel [15]. Final assembly took place at Giessen University, Germany [16] and the system will be commissioned at GSI in a future experiment.

3.3. Target system design and assembly

The principle part of the MNT target system is the main target wheel, shown in Fig. 18. This contains six positions, three of which are dedicated to mounting of thin targets for MNT reactions, two positions are collimation apertures at 15° and 60° that can be used to collimate emissions from a removable ^{252}Cf spontaneous fission source (for offline testing) and one is an open position to allow the principal beam to pass unaltered.

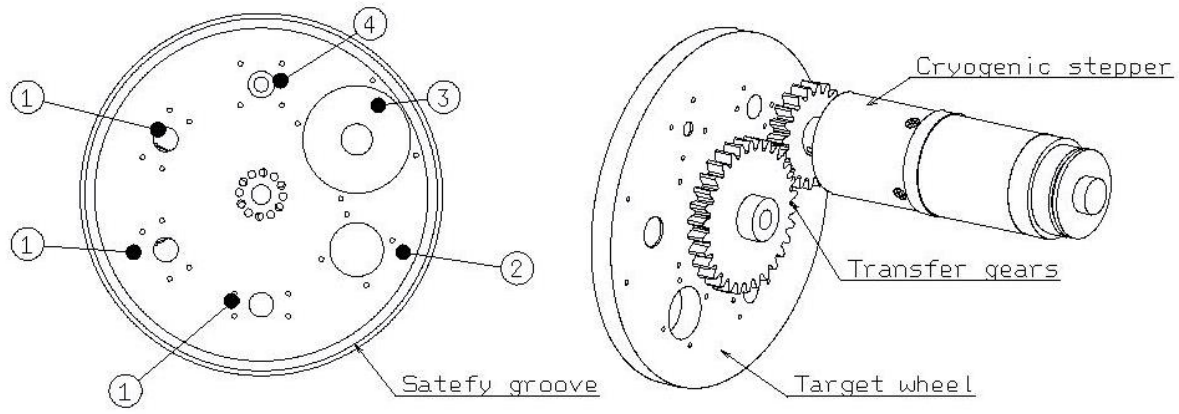

Figure 18: Main target wheel with cryogenic stepper and transmission gears. 1: openings for MNT targets, 2: clear path, 3: 60° collimation aperture, 4: 15° collimation aperture

To perform off-line measurements with the ^{252}Cf fission source, shown in Fig. 19, a special holder was designed into the casing of the target system in which the source can be mounted on a large M30 threaded port.

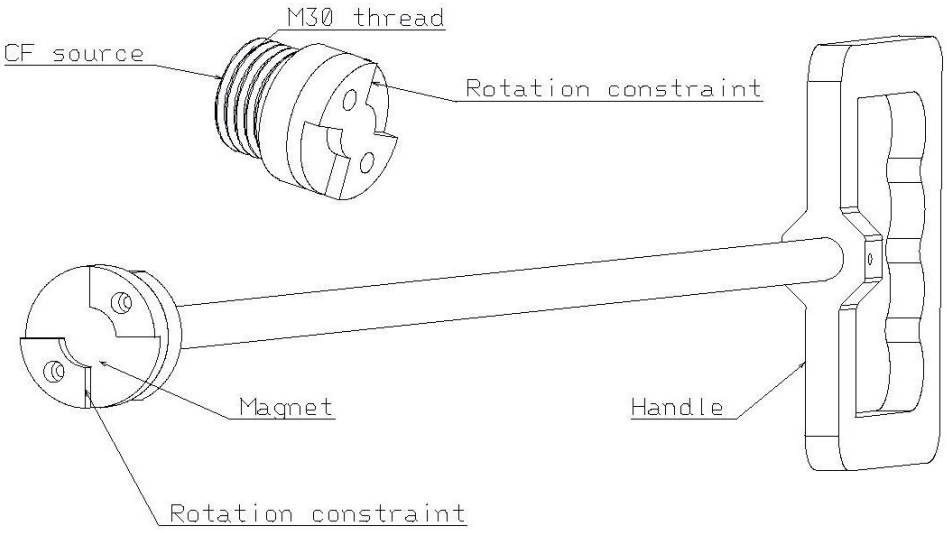

Figure 19: 252Cf fission source casing and safety rod for mounting and unmounting

The secondary component of the target system is the secondary target wheel which is illustrated in Fig. 20. This is a much smaller structure that is assembled inside the DC rings, connected to the back of the target system.

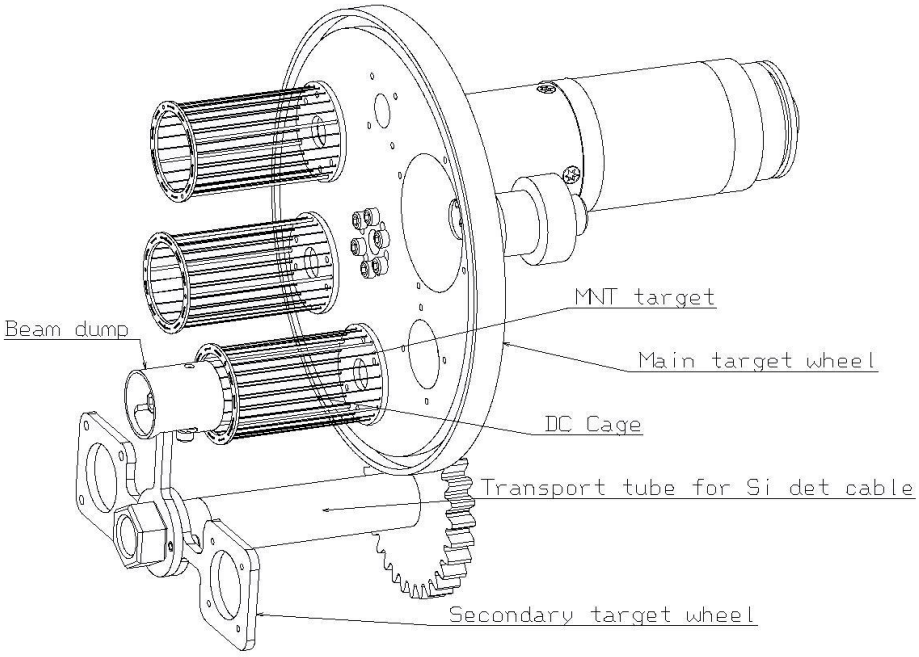

Figure 20: Isometric view of main and secondary target wheels

When the incident uranium beam will irradiate thin MNT targets, most of the primary beam will be absorbed but a small part will penetrate through and will cause helium ionization inside the stopping chamber. To suppress the build-up of space charge, a beam dump positioned at several cm after the targets is required.

Because in MNT reactions, both projectile like fragments and target like fragments are emitted at various angles and do not preserve the incident angle of the primary uranium beam, these MNT fragments will be emitted around the beam dump and will be able to continue into the stopping cell for extraction. To complete this setup, small DC cages are mounted on the

primary target wheel that shield the space-charge region between MNT target and beam dump as to suppress the helium ions from leaking into the system.

Thirdly a system of transfer gears is used to transfer torque from the user to the secondary target wheel. The full transfer system is presented in Fig. 21.

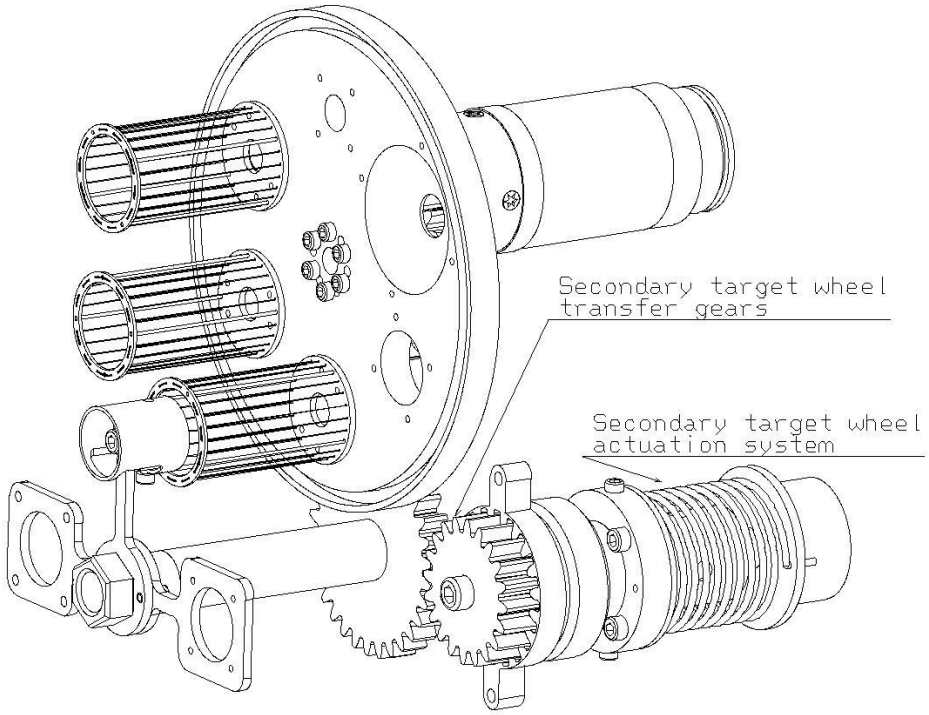

Figure 21: Isometric view of both primary and secondary target wheels with transfer gears and actuators

An important radiation safety requirement of the system is to have an interior chamber that is encapsulated. This is due to the high activity of around 10 MBq of the ^{252}Cf fission source for when it will be used for off-line testing.

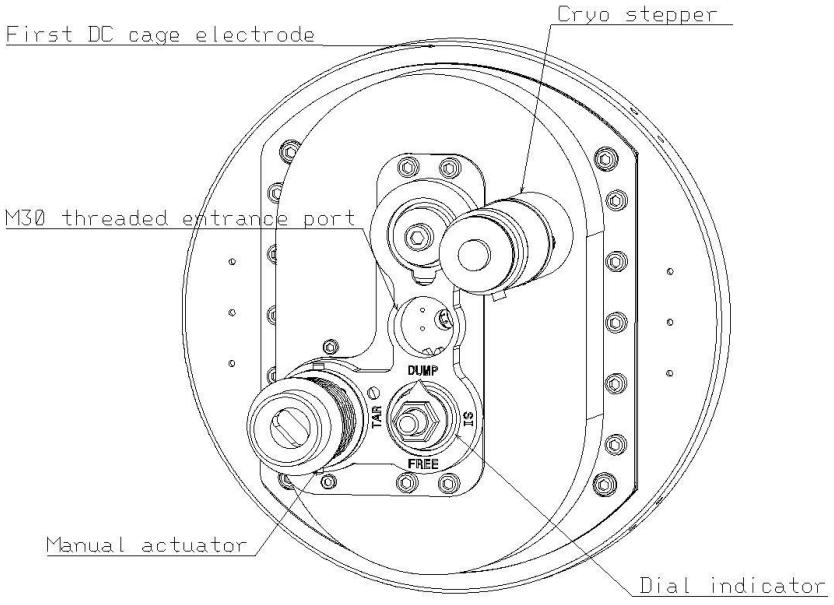

Figure 22: Assembled cryogenic target system for MNT reaction studies

The overall constructed assembly is presented in Fig. 23.

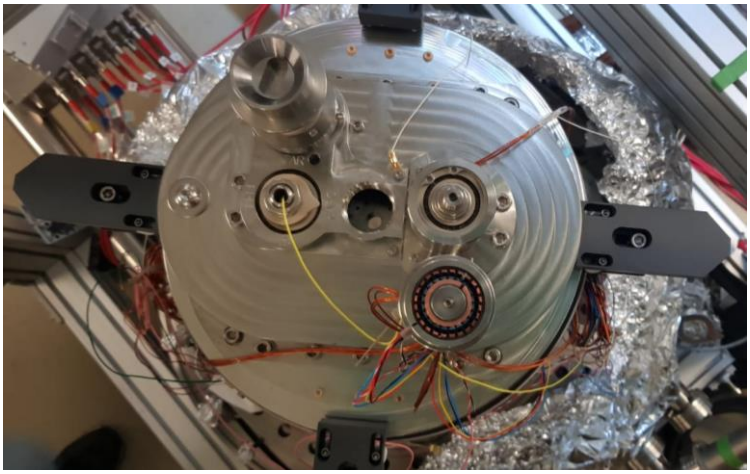

Figure 23: Target system with modifications installed on the DC cage

After final modifications, the target system was mounted to the shortened DC cage after it was tested to work correctly. A control software for the cryogenic stepping motor was designed in the LabView development environment and the overall system is ready for cryogenic testing by liquid nitrogen immersion and if successful will be mounted inside the Cryogenic Stopping Cell for the future MNT reaction experiments planned to be carried out at GSI.

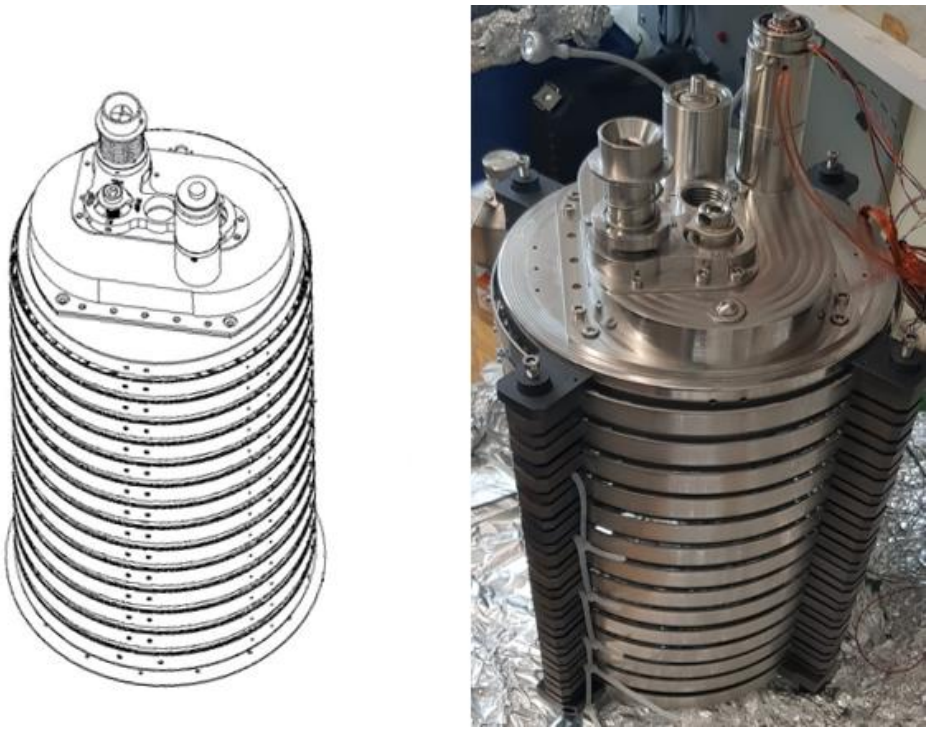

Figure 24: From CAD design to functioning system

3.5. Target wheel operation modes

The most important mode of operation is for MNT reactions. This configuration is illustrated in Fig. 25. For this the entrance to the target wheel is cleared such that uranium

incident ions are used, the first target wheel is in either the fourth, fifth or sixth positions (thin targets positions) and target wheel two is in beam dump position. DC cages for space charge suppression are mounted between carousel one and two. MNT fragments will be produced at various angles with respect to incident beam direction and they will bypass the beam dump and continue into the system.

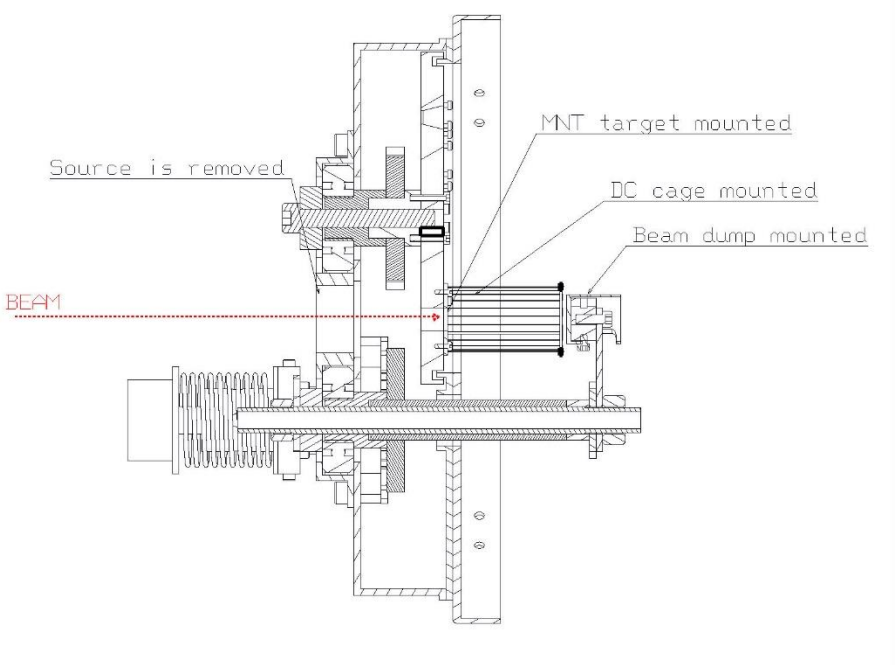

Figure 25: Target wheel in MNT configuration

The efficiency of various DC cages has been studied in order to optimize their design. When an incident pulse of approx. 10^7 ions of ^{238}U enters the stopping chamber to interact with the MNT target, around 85% of the incident uranium ions will penetrate this target and the beam dump is used to prevent them from continuing inside the stopping cell. Regardless, the high kinetic energy of these ions will ionize the helium between the MNT target and the beam dump and can create significant space charge. The amount of space charge produced for a beam pulse of 10^7 ions has been simulated in Fig. 26.

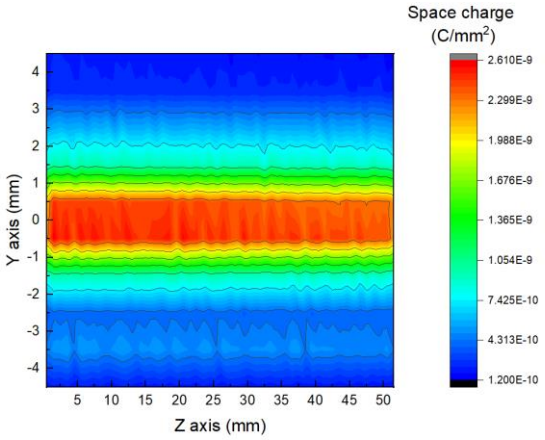

Figure 26: Space charge produced between the MNT target and the beam dump

The space charge produced has been calculated for every cubic mm inside this stopping volume. The purpose of the DC cage is to capture the helium ions such that they do not leak into the bulk of the stopping cell volume. It can accomplish this in two ways. Firstly it can serve as a negative electrode (compared to the space charge itself) to provide a guiding path for the helium ions towards it and secondly voltage drops can be used to create additional fields that can guide helium ions into the beam dump or another electrode used for neutralization. Four geometries have been studied, presented in Fig. 27. Three geometries use a DC cage for helium ion containment, and one uses only the beam dump for comparison.

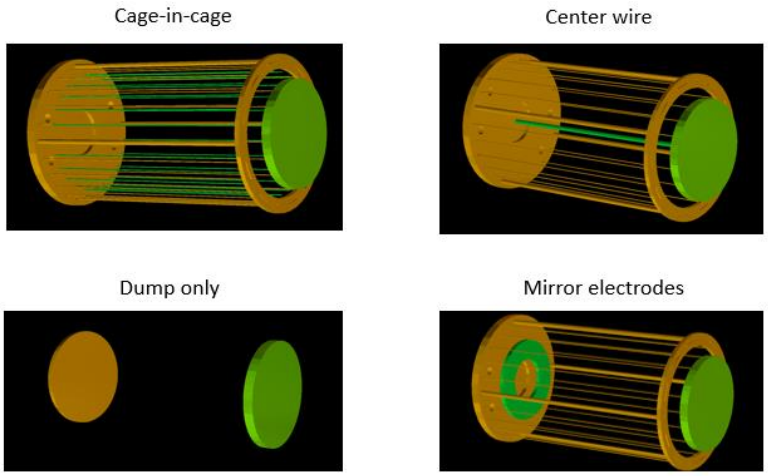

Figure 27: Various designs for the DC cage space charge suppression

The containment efficiency has been studied for each variant for different amounts of space charge, based on the space-charge distribution. These results are shown in Fig. 28.

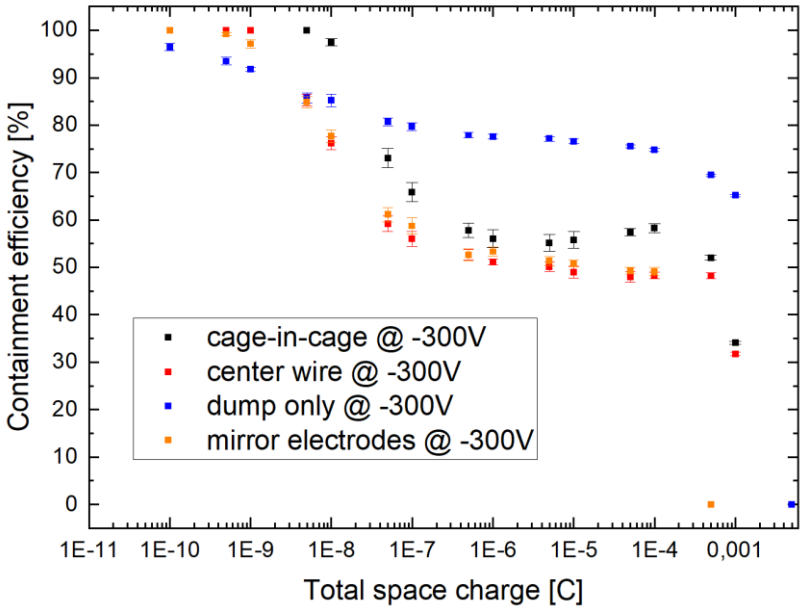

Figure 28: Space charge containment efficiencies for different variants of the DC cage with negative bias applied

Based on the results discussed in this chapter, an article is in advanced preparation and is planned to be submitted to Nuclear Instrument and Methods, section B.

Conclusions

This experiment is a collaboration between three research institutes and the Giessen University. The solution presented, together with the CAD design of the mechanical system and technical execution drawings were provided by ELI-NP, Romania, myself being the principle investigator. Manufacturing of the physical components was executed at Soreq Nuclear Institute, Israel. Troubleshooting and final assembly was done at the Giessen University, Germany, together with final procurements of smaller components like screws, compression spring, magnet etc. The MNT experiments will be carried out at GSI. The mechanical engineers at Soreq did an excellent job manufacturing all components and the laboratory provided at Giessen University was well equipped to perform the necessary troubleshooting. This entire endeavor is ultimately a team effort and the main result that was obtained is a system that works and a fruitful collaboration between our four respective teams. I would especially like to thank Daler Amanbayev and Lizzy Gröf from the Giessen University and David Benyamin from Soreq Nuclear Institute for being instrumental in completing this work.

Chapter 4: RF Carpets

4.1. Context

Electro-optical elements are used to transport and analyze different types of ion beams for different purposes and across many types of devices. Such devices can range from simple mass spectrometers used to define the beam type by mass to complex particle accelerators. At the basic level, electro-optical elements are used for three broad types of applications. They can be used to generate different types of ion beams, for example ion sources, they can be used to transport and manipulate different types of beams from one location to another with different efficiencies and they can also be used to process and analyze these ion beams. The ion beams can be characterized by their species, their mass distribution, energy distribution, charge distribution, envelope, and emittance etc.

A fundamental problem in beam handling is that any kind of optical element has a property called acceptance that represents the maximum emittance that a beam transport system can transmit [17]. In any kind of ion source must fulfill two important tasks, namely ion generation and ion extraction. Usually an ion source is coupled with an Einzel lens to keep the shape of the ion beam, thus preventing its emittance from exploding. However, in an ion source where ions are generated with a wide momentum spread, for example in a secondary reaction ion source, a wide acceptance is needed by the beam transport system to be able to extract and produce a usable ion beam. This is the main application for radio frequency (RF) carpets and RF funnels. [17]

These optical elements can take as input a population of ions with a wide momentum and energy spread and can output a beam of low emittance. At the basic level, an RF carpet is a planar arrangement of many metallic strips with different voltages applied on them. These strips can either be arranged in a circular or linear array to accommodate different geometries.

There are three main components in an RF carpet. First, there is a DC guiding field that guides the ions towards the carpet. Second, there is a RF repulsion field that acts at short distance from the carpet and traps the ions above its surface. Third, there is a steering field that concentrate the ions towards an exit nozzle. Usually an RF carpet is placed inside a gas chamber of some pressure. Through collisions with neutral gas particles, ions entering this chamber will be thermalized, thus the gas acts like a velocity limiter. If electric field lines are present within the volume than these thermalized ions will follow the field lines precisely. Thus, it is possible to extract ions with very wide momentum and energy spread using an RF carpet placed inside a gaseous chamber. This is of significant interest for the production of secondary ion beams through nuclear reactions because these secondary ions are usually generated with wide momentum spread, high charge, high kinetic energies etc.

At ELI-NP a Radioactive Ion Beam (RIB) beamline will be built within the upcoming project for the extension of its experimental building towards the IFIN-HH nuclear reactor, which has been recently decommissioned. This facility will use the high intensity gamma beam, tuned to the Giant Dipole Resonance region of ^{238}U (~10-18 MeV), to generate photo-fission fragments in a stack of ^{238}U targets placed in the center of a gas cell [18]. After thermalization in the gas, these heavy ions are transported by a combination of several types of electric fields

and multiple supersonic gas jets to the cell exit. Central to this experiment is the capture and extraction of these heavy ions using an RF Carpet. The beamline continues with a Radio Frequency Quadrupole (RFQ) [19] for beam formation and a powerful ($m/\Delta m > 5 \cdot 10^5$) Multiple Reflection Time-of-Flight mass spectrometer that selects exotic neutron-rich nuclei for an extensive experimental program [20].

Arriving from this experimental program is the necessity to develop and produce a custom solution of RF Carpets to be used for beam extraction and formation. Because of this, various RF Carpets concepts has been designed and investigated.

4.2. The ELISOL facility at ELI-NP

The ELI-NP facility can provide high-brilliance gamma beams, which will provide us with a new tool for nuclear research [21]. Since the energies of these gamma rays will cover the domain of the huge dipole resonance, it could be suitable for the production and research of fission fragments through photo fission reactions.

In order to study the Zr-Rh refractory elements (A~100) and the rare earth elements (A~140), an experimental procedure for generating neutron-rich radioactive ion beams (RIB) was proposed [20]. To this end, the ion-guided isotope separation online technology (IGISOL) together with the high-brilliance gamma rays at ELI-NP will be used as the main beam.

In ELI-NP HADO-CSC, the main gamma rays will hit multiple ^{238}U thin targets, triggering giant dipole mechanism, and causing the release of photo fission fragments. Once the ^{238}U nucleus splits, the photo fission fragments can have a kinetic energy of 20-100 MeV (depending on the mass) and a very wide momentum spread [22]. In Figure 29, showing the ELI-NP cryogenic stopping cell demonstrator, this happens in the lower chamber denoted by chamber 1.

The chamber is filled with helium at 300 mbar and a temperature of 70 K. The stopping power of the gaseous medium will thermalize all fragments within 10 cm [18]. As an inert gas, helium is an excellent choice because it has a high ionization potential. The charge of the fragments should not be neutralized by charge exchange with residual gas impurities, thereby rendering the electric field extraction ineffective. Therefore, the chamber must be filled with ultra-pure helium gas and kept at a low temperature to freeze most of the impurities to the wall.

By colliding with neutral gas particles, the fission fragments are thermalized, and the gas imposes a speed limit due to the stopping power. If there are electric field lines within the volume, any ion will follow the electric field lines accurately. Therefore, fragments with a very wide distribution of kinematic parameters can be extracted if they retain at least 1^+ charge. In this extraction method, the RF carpet acts as a collector of slow ions.

Once the fragments are thermalized, a DC guiding field is used to direct them towards the extraction side of the chamber. These field lines fill the entire chamber and will have a strength of around 100 V/cm. The extraction side of the chamber is equipped with RF carpets. This is used for two purposes. First, the RF carpet will stop incoming fragments in an RF trap by essentially applying a small repulsion force at a close distance to it. The fragments will enter an equilibrium between the carpet RF repulsive field and the DC guiding field, that is pressing them against the carpet.

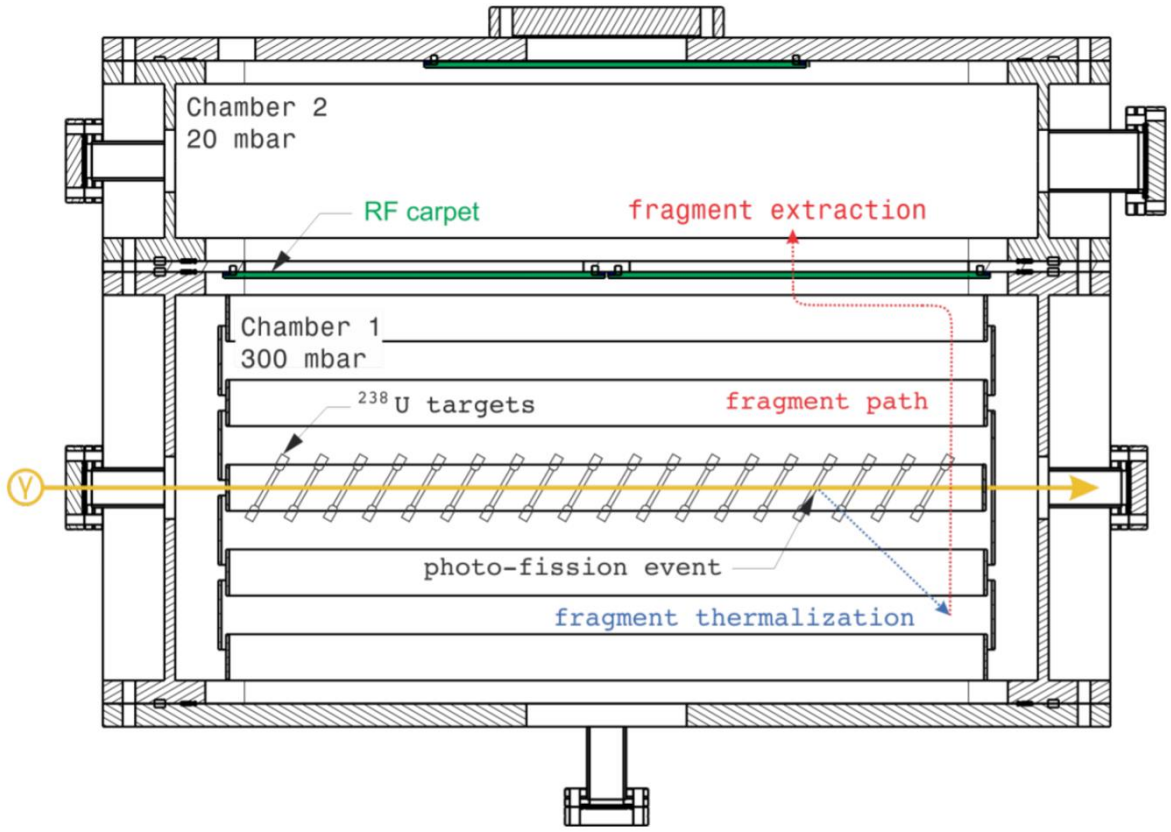

Figure 29: Illustration of cryogenic stopping cell used to create radioactive ion beams using the (γ,f) reaction. In this illustration, yellow line represents the primary gamma beam and its direction and the blue and red dotted lines represents the path of fission fragments during its three flight phases (thermalization, drift and drag)

4.3. RF Carpet simulations

The two most important parameters to be considered for the extraction of photo-fission fragments with the use of RF carpets are the extraction efficiency and the extraction times. Therefore, the RF carpet must be simulated as accurately as possible to determine a good design and estimate the extraction parameters. SimIon 8.1 [23] is an excellent software for electro-optical simulation. Complex geometries can be produced, and the use of Lua scripts allows the simulation of complex physical behaviors, such as ion-gas collision models.

To simulate this, ions were generated at the end of the RF carpet, and a DC field was applied between the outermost electrode used as the anode and the innermost electrode used as the cathode. The field is divided equally between the remaining electrodes to form equipotential. We recorded the flight time and calculated the ion speed for different DC steering fields. These results are shown in Figure 30. For these simulations, an RF frequency of 6 MHz and an RF amplitude of 130 V were used.

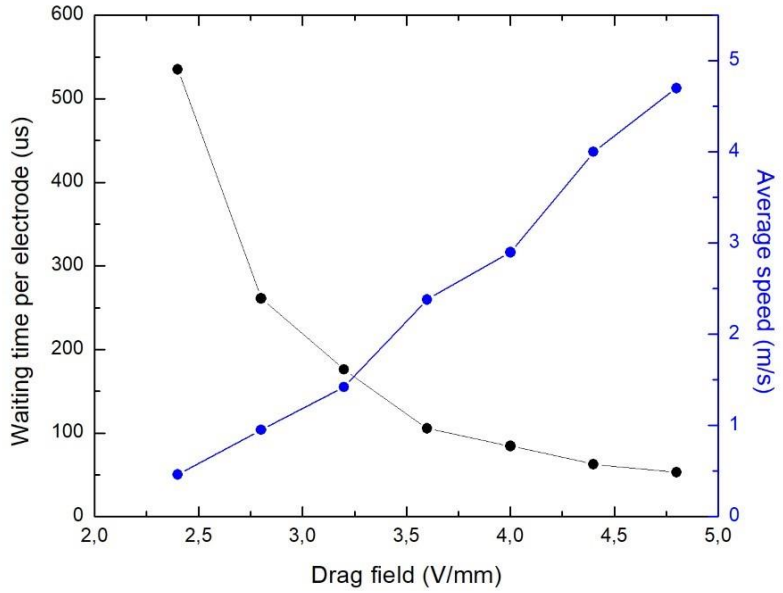

Figure 30: Ions average speed above the RF carpet and average waiting time per electrode for different drag field voltages

A limiting factor in the Cryogenic Stopping Cell performance is the ability of the RF carpet to capture ions of different incoming speeds. In the first simulation investigating the ability of the RF carpet to hold ions above it, the ions entered at an average velocity of approximately 17 m/s. The simulation was repeated adding an airflow component that increases the ion velocity.

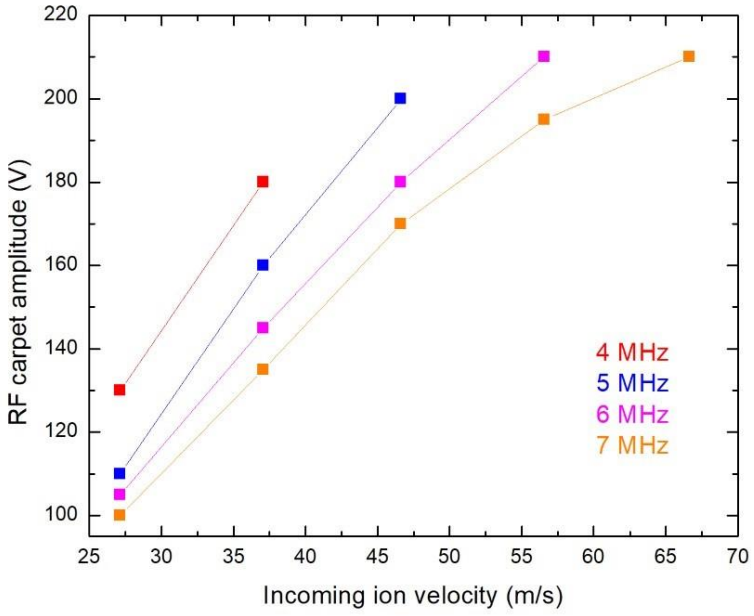

Figure 31: RF carpet voltage amplitudes needed to catch ions at different incoming speeds

The calculated ion speed based on the time of flight is presented in Fig. 32. Also in this figure is displayed the calculated average waiting time, which is the time it takes for the ions to progress one electrode towards the extraction nozzle.

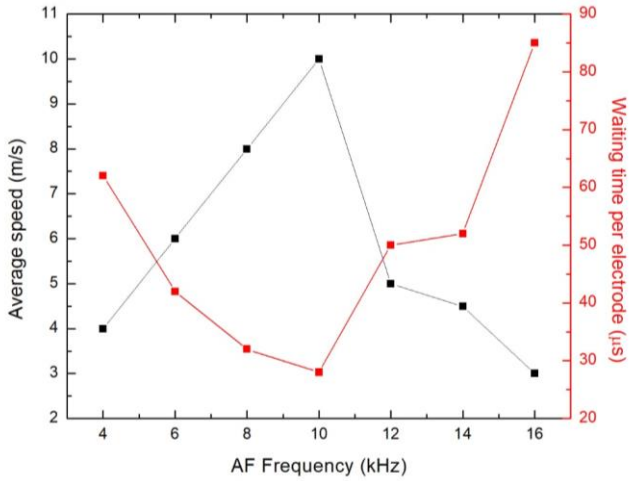

Figure 32: Ions average speed above the RF carpet and average waiting time per electrode for different AF frequencies at 3V

4.4. Extraction time calculations

The simulations done thus far, allowed to specify the working parameters for the extraction of fragments using RF carpets using two extraction methods, DC drag and traveling wave. For simplicity, we will consider the case of one RF Carpet with a diameter of 25 cm and with 500 electrodes (4 electrodes/mm) placed inside a stopping cell with cylindrical geometry and a height of 200 mm.

A thin ^{238}U target placed in the center of this cylindrical volume is considered. Irradiated with a primary gamma beam of $5x10^{11}\gamma/s$ and energy in between 12-18 MeV, approx. $2x10^{6}$ fission fragments/sec will be produced. These fragments will be emitted back-to-back in random directions [20]. The initial energy of photo fission fragments will be around 20-100 MeV, and the charge will be between 10-20q. The entire volume is filled with 300 mbar of pure helium at 70 K. Through elastic collisions, the fragments will thermalize very quickly, about 50 ns, and end with kinetic energy ~ 1-2 keV and charge q = + 1. After thermalization, the fragments will have displaced about 100 mm from the ^{238}U target in a random direction. We define the RF carpet as being in the upper position and a repulsion field coming from positive electrodes in the lower region. The geometry is illustrated in Fig. 33.

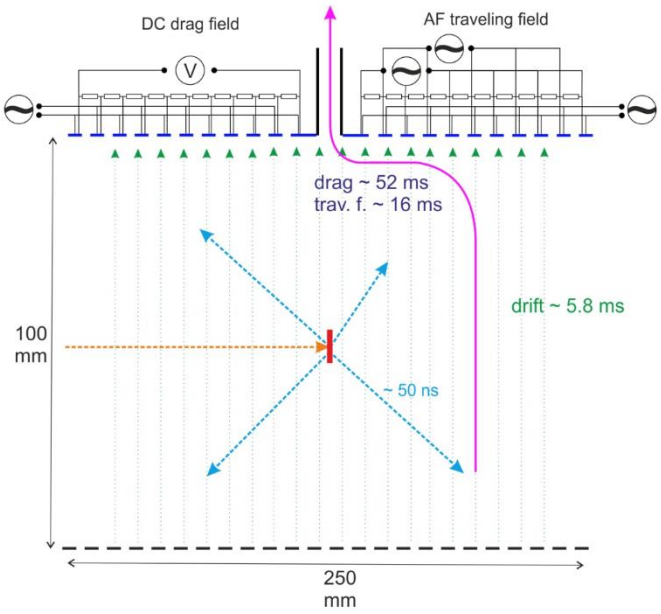

Figure 33: Geometry used for simulations with repulsion electrodes in the bottom, 238U in the center and RF cappet in the top

The easiest way to calculate the average extraction time using these travel velocities is to calculate the travel time based on the travel length for each emission angle. As a good approximation, all ions will be thermalized during a travel length of 100 mm within the gas. Assuming for simplicity these ions are generated from a point-like source, this corresponds to the spherical coordinate r. Since we are evaluating placement in the center of the RF carpet, and the carpet has a cylindrical geometry, the θ coordinate can be ignored. The φ coordinate takes values from 0^0 to 180^0. The travel length and travel time are calculated for each emission angle.

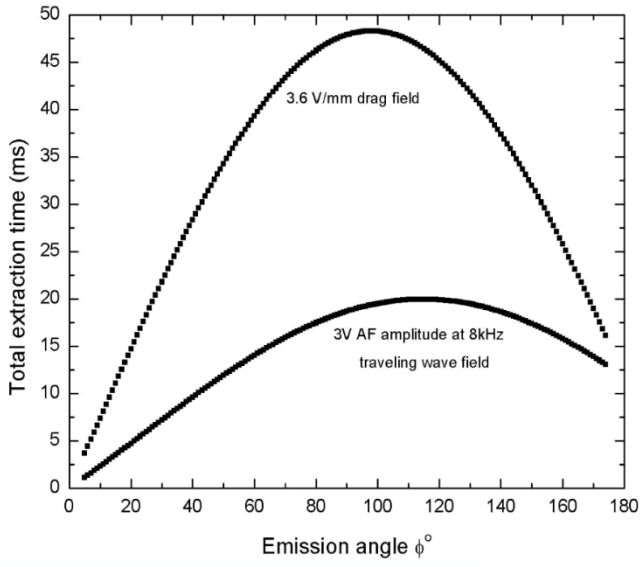

Figure 34: Fragment extraction time calculated as a function of emission angle; each data point represents a group of ions emitted at a certain angle and the time it takes to extract them

Figure 34 shows the relationship between the total travel time and each emission angle. The time it takes for these ions to reach the extraction nozzle is calculated. These calculations

are done for both DC drag and travel wave extraction methods. The total extraction time is given by the thermalization time, drift time and hover time above the RF carpet.

For studying, a chamber smaller than the planned HADO-CSC for ELI-NP has been simulated. This chamber consists of two gaseous chambers placed on top of each other, connected through two small 0.6 mm diameter nozzles. It consists of three RF Carpets for ion extraction, two in the bottom chamber and one in the upper. The reason for using an orthogonal extraction ion chamber is to decrease extraction time. Unlike the cylindrical stopping chamber in which ions are introduced from one end, traveling axially along the chamber and extracted from the other end, in an orthogonal chamber ions are entering parallel to the placement of the RF carpets and as soon as they thermalize, they are guided towards them and extracted. This is further explained in Chapter 5. The system is build like a ladder, the first chamber thermalizes and extracts ions at a higher pressure into the second chamber where pressure is reduced so mobility is enhanced, but because ions enter this chamber through the RF carpet nozzles, they enter with low emittance and are easier to guide towards another RF carpet that handles final extraction.

The small demonstrator system consists of two chambers, each chamber having a rectangular geometry with internal dimensions of L x l x h = 500 x 250 x 250 mm. Both chambers are with identical geometry, as shown in the left side of Fig. 35. The simulated ion transport through this system is presented in the right side of Fig. 35.

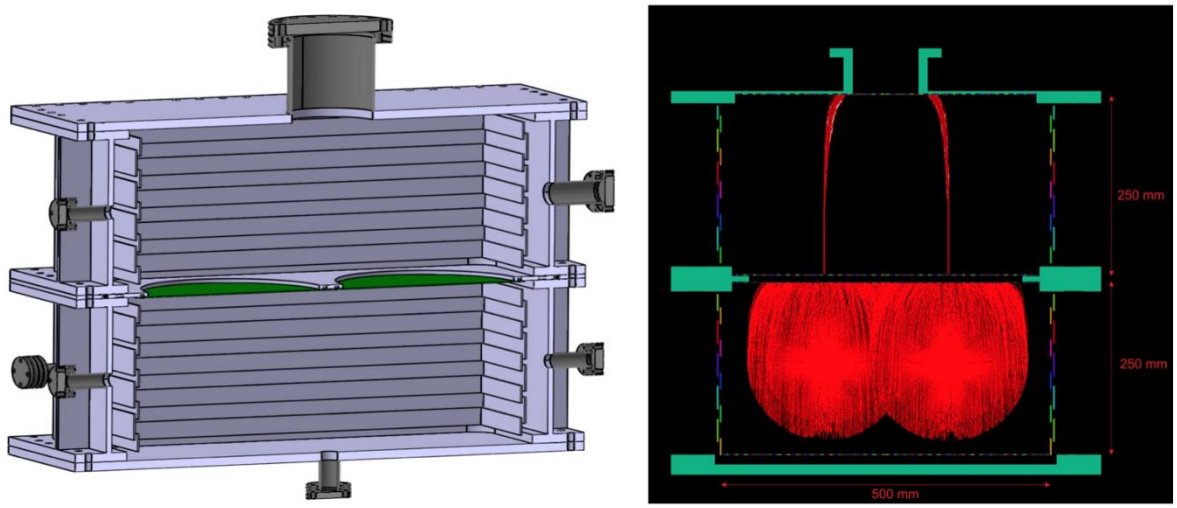

Figure 35: Left: 3D CAD design of CSC Demo; Right: Simulated ion transport through the system

Based on our simulations, we can state the following parameters:

- Chamber is filled with helium gas at 70 K
- The drift repulsion field is 10V/mm and fragments travel through the gas with approx. 17 m/s
- The RF carpet has electrodes with 0.25 mm pitch, operates at 6 MHz and 130 V_{RF}; at these values, it can catch incoming ions with speeds of up to 32 m/s
- If we use a DC drag field of 3.6V/mm, a fragment speed of 2.38 m/s is reached on the surface
- If we use traveling wave at 8 kHz and 3V amplitude, a fragment speed of 7.81 m/s is reached on the surface

4.5. RF Carpet construction

RF Carpets are constructed using the technology which is used to produce Printed Circuit Boards (PBCs) [24]. This technology uses an insulating material of various properties, typically a FR4 material [25] or something more sophisticated like Rogers 4000 or I-Tera [25] and on top of this insulating material an electrical layer made from copper of various thicknesses can be applied. By using either etching or lithography, the copper layer can be shaped in various geometric forms. A typical PCB is composed of two layers, meaning it has an upper and lower conductive layer and a dielectric in between. More layers can be constructed by lamination, for example 4 layers by having two more hidden layers, inside the material.

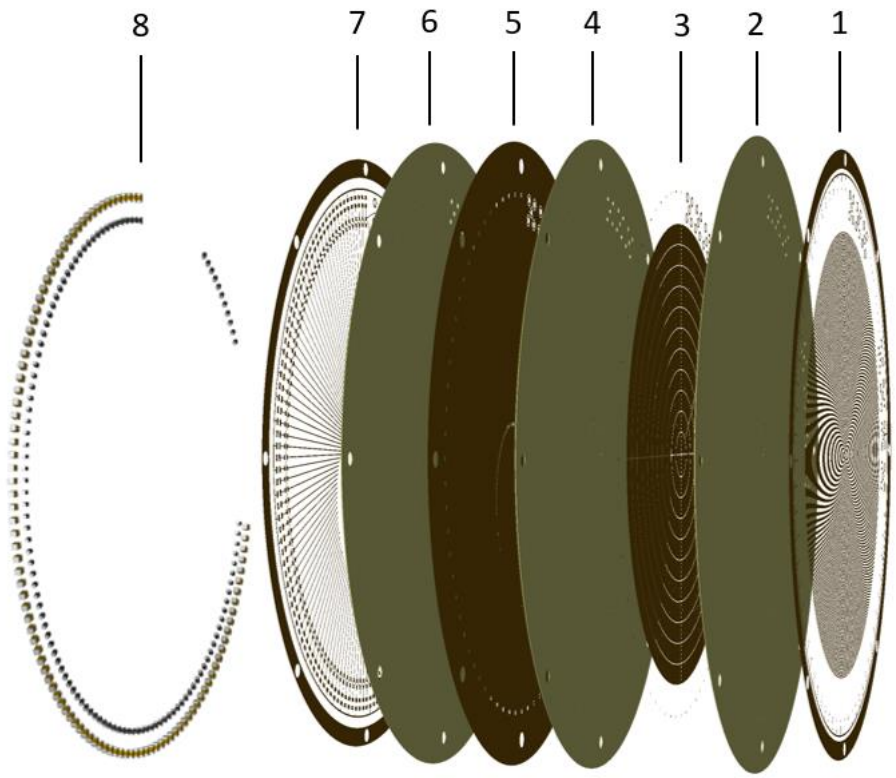

Figure 36: The layers of an RF carpet. 1: Top layer, 3: inner hidden DC rings, 5: inner hidden ground, 7: bottom connection layer, 8: electronic components, 2,4,6: insulator

To create the electrodes of an RF carpet, the top copper layer is arranged in a series of geometric circles. The circles consist of tracks (a thin copper segment) that are spaced apart at different distances. In principle, the more electrodes can be constructed per mm, the higher the estimated RF repulsion force, and higher overall extraction efficiency can be realized. There is a physical limitation in the manufacturing capability of such PCBs and using different technologies, a minimum track width can be reached. Usually this is also the minimum distance between two electrodes. A microscope image of the copper tracks on the surface on an RF carpet is shown in Fig. 37.

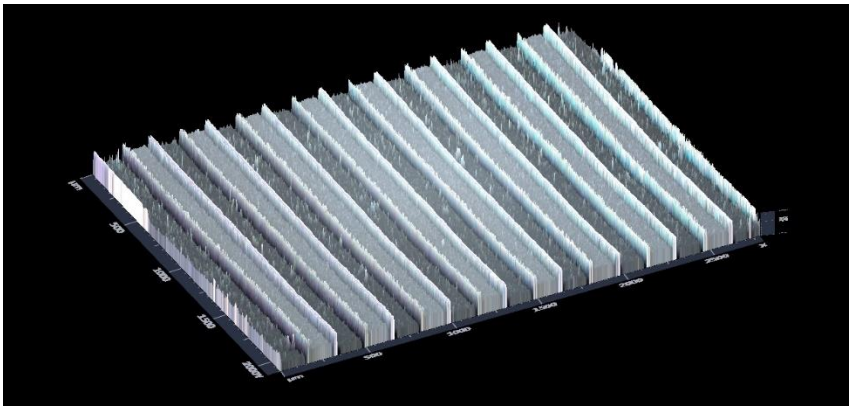

Figure 37: 2.5D microscope image of the surface layer of an RF carpet

4.6. Spiral RF Carpet

The use of traveling wave transport can be beneficial because of two reasons. First, it can enable faster ion transport leading to shorter extraction times. Second, it eliminates the need to use electronics onboard the RF Carpet. This is a very practical matter, because it makes carpet construction simpler and eliminates one potential point of failures. An RF carpet needs to function in a cryogenic environment and small electronics components do occasionally break down. In a large RF carpet with hundreds of small components arranged in a tight geometry, debugging is challenging. These electronic components are also a source of heat, especially if they malfunction. By using only six modulated signals to drive the ion capture and extraction, the RF carpet itself is simplified.

Another practical matter is important to consider. Ideally, by increasing the density of electrode on the surface, the capturing repulsion field can be increased which can lead to better extraction efficiency. On a different aspect, the driving voltages can be lowered which can lead to lower heat emission, something that is essentially important to maintain the low temperature inside the stopping cell. The main limiting factor while trying to increase electrode density is a practical one, namely that the vias are always larger than the track width of the copper electrodes. A possible solution to overcome this problem is to eliminate the vias altogether. This is possible by arranging the top layer electrodes in a spiral geometry, essentially replacing several electrodes all at once with a long spiral. For the realization of this idea, several key factors need to be considered. First, if we only consider the RF repulsion field, two alternating signals with a 180^{o} offset (opposite in direction) needs to be applied on all electrodes sequentially, meaning the first RF signal is applied to all odd numbered electrodes and the second RF signal to all even numbered electrodes. Circular electrodes are arranged concentrically at a fixed pitch, for example one electrode at every 0.5 mm step. We can replace all the electrodes on which RF signal 1 is applied with a single long spiral electrode. This spiral will have an origin point at the edge of the active area and will end somewhere close enough to the extraction nozzle. The spiral will have a pitch which is twice the pitch of the carpet, for example 1 mm. We add another spiral for the electrodes of RF signal 2 but the origin point is symmetrically rotated at 180^{o} such that the two spirals are now nested. For the system to work, at any point on the active area the distance between the edges of the first spiral and the second spiral must remain the same. This geometry works because at the microscopic level, the ions feels no difference between a spiral geometry and a circular one. This is because the curvature

of the spiral is insignificant from the point of view of the traveling ions. However only two spirals could only be used to capture ions, they could not extract them. Using a DC guiding field will be impossible because we cannot apply a voltage drop on a continuous electrode. However, the geometry lends itself as being very practical for traveling wave transport. The minimum requirement is to have four spirals nested together, each one offset by 90^0 with respect to the origin of the carpet. A traveling wave signal is applied on these four spirals and the wave travels inwards from the edges of the active area towards the center extraction nozzle.

The spiral geometry was simulated in SimIon 8.1 and the results are very promising. The system overall functions with the same parameters as a circular traveling wave carpet. From these simulations it has been deduced that the area of the operational regime increases directly proportionally with the increase in pressure but decreases proportionally with the applied push field and the traveling wave amplitude. The spiral RF carpet behaves like a circular electrode RF carpet from the point of view of these operational parameters and its ability to capture ions. Based on the results discussed above, an RF frequency of 3 MHz at an RF amplitude of 60V has been chosen because this provides the largest operational area. Using these values and a pressure of 30 mbar and a push field of 1 V/mm, the extraction times for a carpet with a diameter of 250 mm are computed for various travel wave frequencies and travel wave amplitudes. These results are shown in Fig. 38.

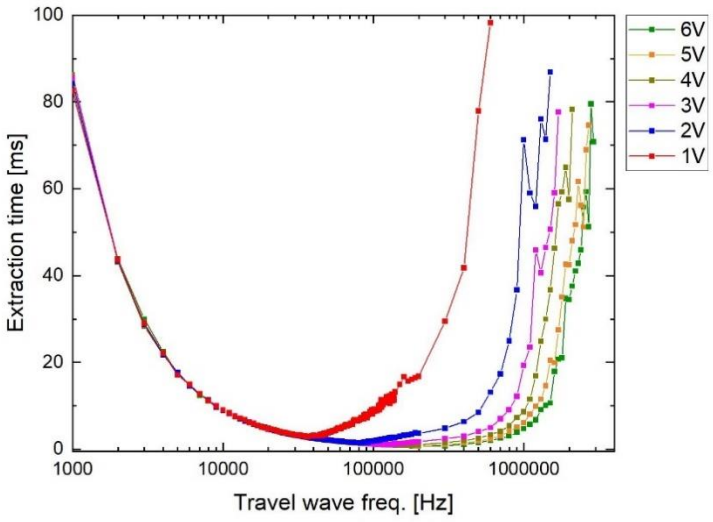

Figure 38: Ion extraction time for a spiral RF carpet with traveling wave extraction at different frequencies and amplitudes

4.6.2. Spiral RF Carpet construction

The carpet shown in Fig. 39 has spiral geometry with 4 spirals, only a top spiral layer and a bottom ground layer and has five electrical connections. Each spiral has its own electrical connection, which is not shared, and the extraction nozzle has one. The spirals have been measured to produce around 0.49 nF of capacitance between them and they each have around 21.5 Ohms of resistance.

Figure 39: Electrical testing of spiral RF carpet

A 2.5D microscope image of the central extraction nozzle and the terminations of four spirals is shown in Fig. 40. Although the spirals are long electrodes, the resistance remains negligible and does not create electrical problems. There are however other practical problems that might appear, because of the length of these electrodes, small manufacturing defects or mishandling could create defects.

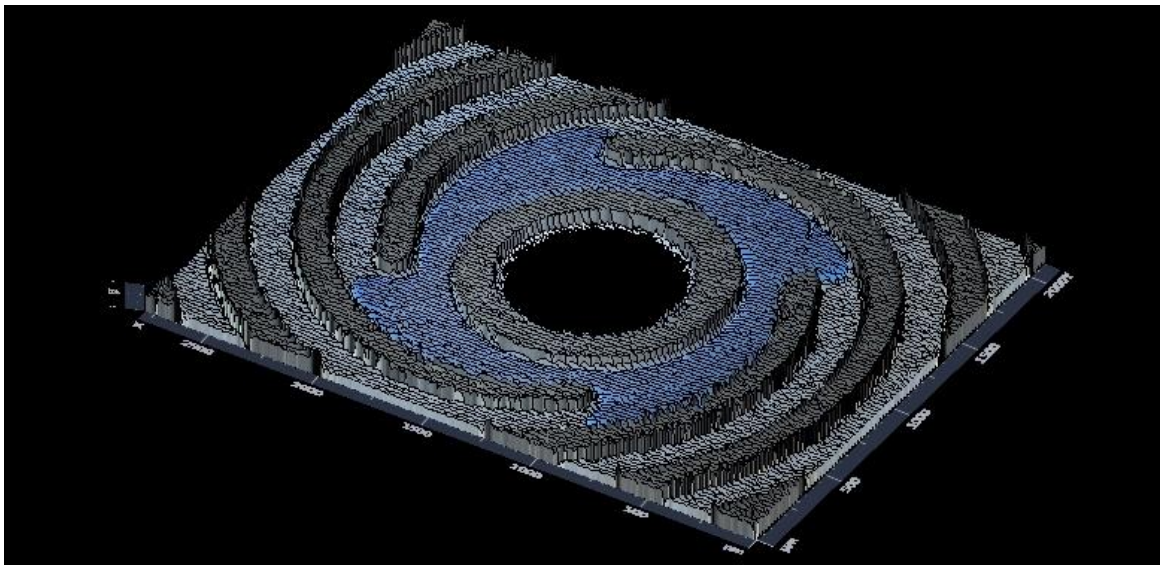

Figure 40: 2.5D microscope image of the extraction nozzle of a spiral RF carpet

This spiral RF carpet is a prototype used to investigate how this geometry behaves experimentally. The spiral geometry could potentially be used to produce RF carpets with high electrode densities because it can eliminate the need for vias and simplify overall construction.

Based on the results discussed in this chapter, one article was submitted to the Scientific Bulletin of the Politehnica University of Bucharest, section Mathematics and Physics and a second article is in advanced preparation and is planned to be submitted to The Journal of Mass Spectrometry.

4.7. Conclusions

RF Carpets are relatively new concepts that replaced the older RF funnel. They are sophisticated devices and used for ion trapping and extraction and can potentially be used in many different applications, such as mass spectrometers, ion detectors and ion extractors. The working of a circular RF carpet has been investigated using ion-optics simulations for various circumstances to be used for the upcoming ELISOL facility. During these investigations, a novel RF carpet concept was proposed, the spiral RF carpet, and ion-optics simulations tested the new geometry as being viable. If successful, it will offer several advantages compared to the classic circular electrode geometry, the most important being the possibility of leading to increase electrode density which should yield higher extraction efficiencies and lower power consumption. A spiral RF carpet was constructed for testing purposes and it will be used in the upcoming RF carpet testing system, presented in the next chapter.

Chapter 5: RF Carpet testing unit

5.1. Context

The study of the nuclear structure of exotic nuclei presents a worldwide interest, demonstrated by the construction of new radioactive ion beam facilities, for example the Facility for Rare Isotope Beams (FRIB) at Michigan State University [26] and the upgrading of existing facilities, for example the Super Fragment Separator at FAIR, GSI [27]. The in-flight separation method has the potential to produces a wide variety of new and exotic nuclei, however these nuclei will have high momentum spread and require some way to collect them and form a well-defined beam with low emittance and low energy. [28] This is necessary to enable high precision mass measurement and nuclear structure investigations. The most efficient way to produce, collect and extract these exotic nuclei is by using a stopping cell. These chambers are filled with various gases at different pressures and temperatures. They can have different layouts with a single or multi-chamber, axial or orthogonal extraction, but they all use RF carpets as the means to collect and extract these exotic nuclei towards an extraction nozzle where the gas flow takes over and the ions are transported outside the stopping cell.

5.2. Design of an RF carpet testing system with axial extraction

The concept for this system was designed around commonly found equipment and some components which were already available. From a construction point of view, we will further explore the most important components of this system.

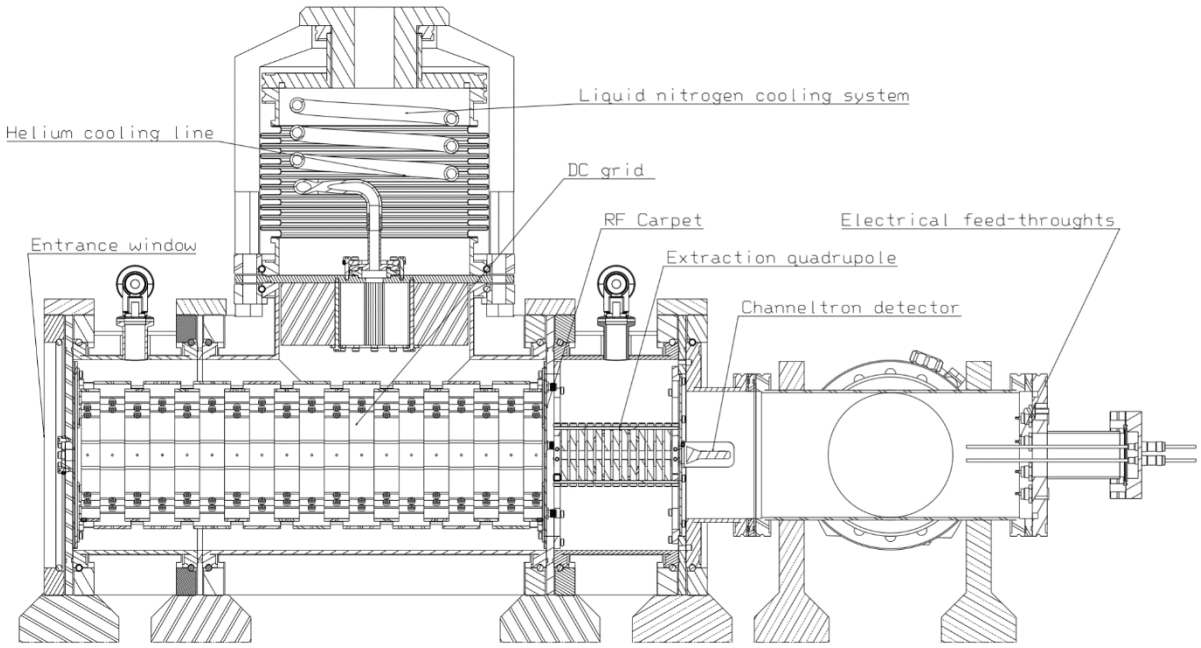

Figure 41: Cut-section overview of the experimental setup

To use this experimental set-ul, a series of driving electronics are required. Three waveform generators with two channels each are used to provide six independent RF signal outputs, four for the RF carpet and two for the extraction quadrupole. Another approach is to split one single signal into two signals of opposing signs by using transformers.

To provide sufficient power to drive the electronics, broadband RF amplifiers are used. Multiple DC voltage sources are required to supply the necessary guiding and acceleration fields. A temperature controller is used to monitor the entire experiment with the use of three PT1000 sensor [29]. High-voltage power supply and a detection chain is used for the channeltron detector. A diagram of the driving systems is presented in Fig. 42.

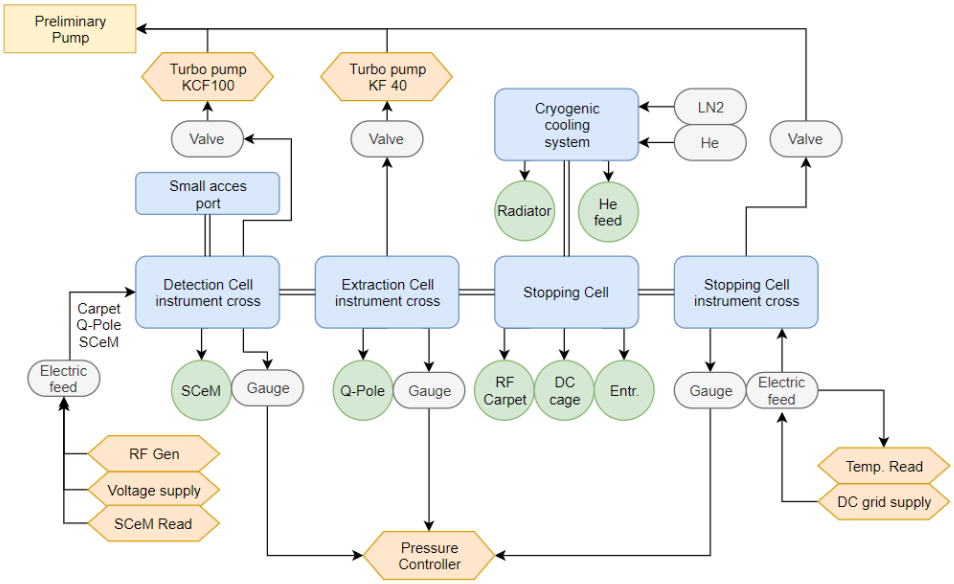

Figure 42: Schematic diagram of driving systems, both electrical and physical (vacuum and thermal)

Lastly, an electrical junction box that distributes the power and provides overcurrent and overvoltage protection is used to ensure the safety of the electronics. The entire experimental assembly with all dependencies, as was proposed for the testing of RF carpets, is presented in Fig. 43.

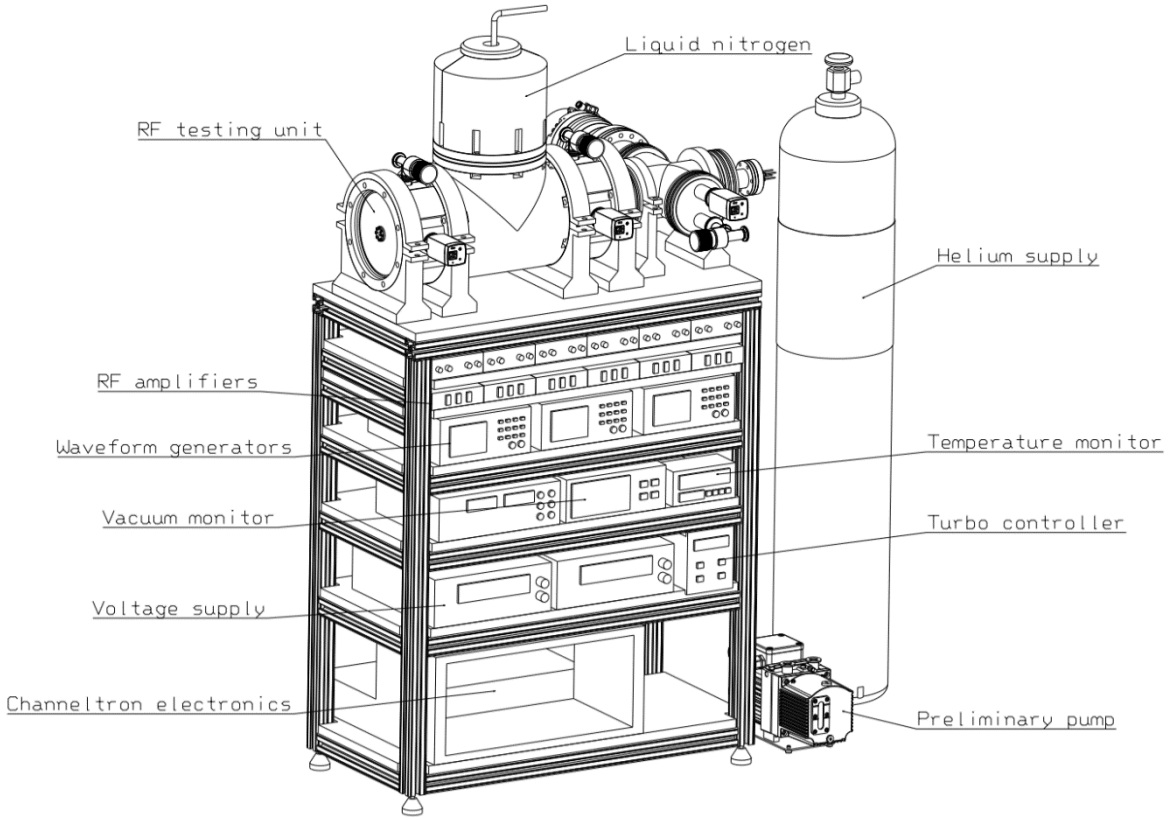

Figure 43: Isometric view of the entire assembly of the experimental set-up for testing of RF carpets

5.3. Design of an RF carpet testing system with orthogonal extraction

A second testing assembly consisting of three chambers was designed that features orthogonal extraction that could be used in the future to simulate a smaller ELISOL experiment and gain important working knowledge towards construction of the real experimental set-up. The components required for the testing of ion capture and transport system are in some way similar to the ones developed in Ch. 5.3, however where they differ is in the DC grid assembly of electrodes which now needs to be constructed orthogonally and not axially. Also, because there are two chambers used for stopping and evacuation of ions towards the extraction quadrupole, two pairs of such electrodes will be required. The chamber will make use of three RF carpets.

The CAD design produced for this experiment is presented in Fig. 44. This new chamber has been constructed and features vacuum system with preliminary pump and turbo-molecular pump, valves and vacuum measurement using 3 gauges. This chamber also makes use of some additional components, such as a gas regulation system, He 5.0 gas supply and a LabView control environment for maintaining the target pressures inside each of the three chambers.

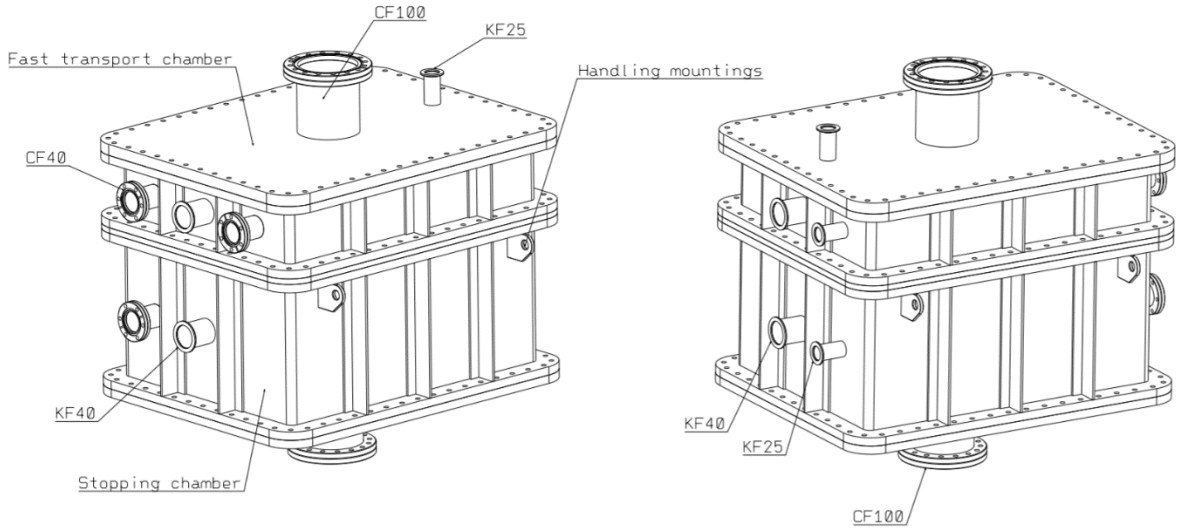

Figure 44: Isometric view of orthogonal stopping cell; Left: Front view, Right: Bottom view

The orthogonal extraction stopping cell, together with vacuum and gas line controllers attached is presented in Fig. 45.

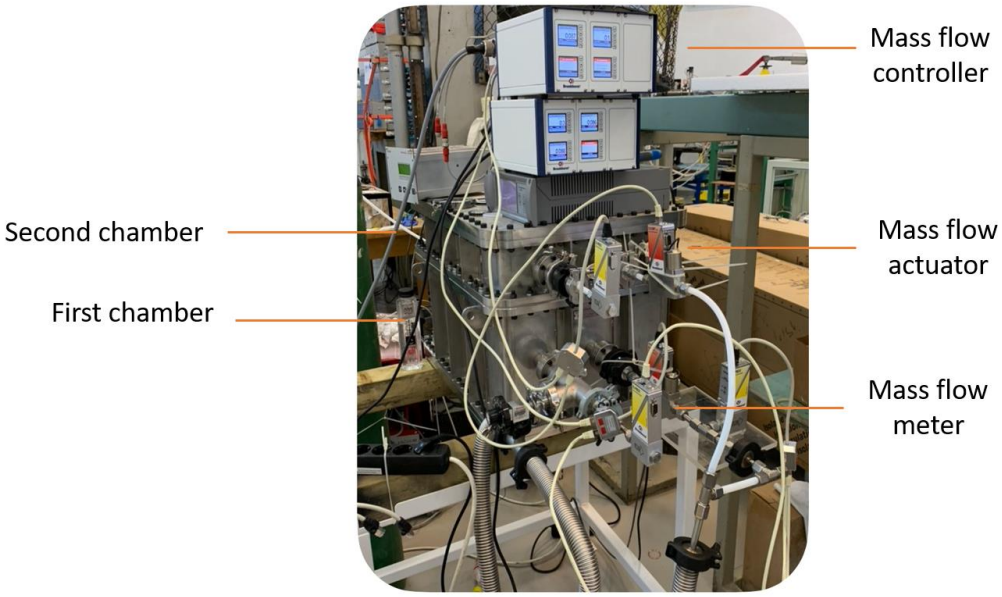

Figure 45: Orthogonal stopping cell with vacuum components mounted

Conclusions

Two RF carpet testing units, one with axial extraction and the other with orthogonal extraction were proposed to serve as a steppingstone towards the upcoming ELISOL facility. Both systems were designed over the course of the last two years with the orthogonal extraction testing system being custom manufactured and the axial extraction system being assembled by standard vacuum components. This smaller axial system is also meant to function as a dedicated testing unit for RF carpets and the various electronic components used for ion manipulation, trapping and extraction.

C1: General conclusions

The developmental work presented in this thesis covers a time span of five years, during which time I have worked and collaborated with research teams at IFIN-HH, ELI-NP and GSI. The thesis was structured around three important systems. At IFIN-HH the external ion beam setup continues to function properly and to this day, there have been numerous beam requests to make use of this capability. At GSI, the Target Wheel has been constructed and will be used in a future experiment aimed at creating radioactive ion beams through multi nucleon transfer reactions. This experiment is scheduled to take place next year. The orthogonal extraction stopping cell used as a demonstrator is currently at IFIN-HH. Vacuum and gas components have been mounted and the chambers ability to hold controlled pressure and gas flows have been proven. The first prototype for a spiral RF carpet is currently at ELI-NP and is waiting testing. Design, manufacturing of some custom parts and procurement of electric components for the RF carpet testing system has been completed and the testing unit is currently being assembled. Once fully functional, it will be tested either with accelerate ion beams at IFIN-HH or with a Thorium source at ELI-NP.

C2: Original contributions

In Chapter 1, the ion-optics simulations presented for the cesium sputtering ion source have been done together with Dr. Doru Pacesila for the 1 MV Tandetron accelerator at IFIN-HH.

In Chapter 2, the mechanical design for the liquid residue sample holder is an original concept and the mechanical design for the beam extraction system, albeit inspired from similar facilities, is a proprietary design that was developed together with Victor Runceanu. Also, the ion optics optimization simulations for the nuclear microprobe electrostatic quadrupole were original, in order to properly focus the beam onto the extraction window.

In Chapter 3, the mechanical design of the target wheel is an original concept. I have also been responsible for providing manufacturing files and I attended the assembly of the manufactured system. I was also responsible for the ion optics simulations of the containment efficiency of the system used to suppress space-charge.

In Chapter 4, the ion-optics simulations of the circular RF carpet has been done to investigate the working principles and capabilities. The layout of the electronic components for the ladder version was inspired from similar RF carpets and the layout of the linearly arranged components is an original idea. The concept of the spiral RF carpet is an original idea, and the ion-optics simulations done with this geometry is also original.

In Chapter 5, both axially extraction RF carpet testing unit and orthogonal extraction demonstrating unit have been conceptually and mechanical designed. The demonstrator unit is based on previous ideas but the design itself is proprietary for both systems.

C3: Perspective of future development

The most important future development is the continuation of the assembling of the RF carpet testing unit. As in all development work, difficulties will arrive since the system itself is complex and involves the usage of low pressure, cryogenic environment, high voltages and precision ion detection, all enclosed in a small volume.

When completed, the system will be used to test RF carpets at ELI-NP and once successful and properly calibrated, it will be used as an invaluable tool to investigate future RF carpets designs. The experience gained from this system will prove invaluable in the realization of the future ELISOL experiment, since the two systems are similar in their basic working principles but vastly different in their size and scope.

Bibliography

[1] Benamar M., „Particle Induced X-Ray Emission Spectroscopy (PIXE),” nr. 10.13140/RG.2.2.10199.83366/1, 2020.

[2] Rauhala E. et al, „An external beam method for ion backscattering,” vol. Section B: Beam Interactions with Materials and Atoms., nr. 6. 543-546. 10.1016/0168-583X(85)90015-1, 1985.

[3] Suzuki K. et al, „Light element analysis of ceramics using in-air ERDA and TOF-ERDA,” vol. Section B: Beam Interactions with Materials and Atoms, nr. 478. 169-173. 10.1016/j.nimb., 2020.

[4] Breese Mark et al, „Applications of scanning transmission ion microscopy,” vol. Research Section B: Beam Interactions with Materials and Atoms., nr. 505-511. 10.1016/0168-583X(92)95524-U., 1992.

[5] B.V., High Voltage Engineering Europa, „High Voltage Engineering Europa B.V.,” [Interactiv]. Available: http://www.highvolteng.com.

[6] Scientific Instrument Services (SIS) by Adaptas Solutions, LLC, 2003-2020. [Interactiv]. Available: https://simion.com.

[7] Amptek, „X-123 Complete X-Ray Spectrometer with Si-PIN Detector,” [Interactiv]. Available: https://www.amptek.com/products/si-pin-x-ray-detectors-for-xrf/x-123-complete-x-ray-spectrometer-with-si-pin-detector.

[8] Jones, Deric P., Biomedical sensors (1st ed.), New York: Momentum Press, p. 177, 2010.

[9] NIST, „National Institute of Standards & Technology,” [Interactiv]. Available: https://www-s.nist.gov/srmors/certificates/611.pdf.

[10] Blumenfeld Y., „Radioactive Ion Beam Facilities in Europe.,” vol. Section B: Beam Interactions with Materials and Atoms, 2008.

[11] Plaß W et al, „FRS Ion Catcher: Setup, Status and Perspectives,” 2011.

[12] Y.X. Watanabe et al, „Pathway for the Production of Neutron-Rich Isotopes around the,” 2015.

[13] Adrian Rotaru et al, „SIMULATION OF CIRCULAR RADIO-FREQUENCY,” vol. 81, nr. 3, 2019.

[14] Constantin Paul et al, „The ELI-NP IGISOL radioactive ion beam facility.,” vol. Section B: Beam Interactions with Materials and Atoms., 2019.

[15] „Soreq Nuclear Research Center,” [Interactiv]. Available: http://soreq.gov.il/mmg/eng/Pages/Home.aspx.

[16] „Giessen University,” [Interactiv]. Available: https://www.uni-giessen.de/welcome.

[17] Rotaru A. et al, „SIMULATION OF CIRCULAR RADIO-FREQUENCY CARPETS FOR ION EXTRACTION FROM CRYOGENIC STOPPING CELLS.,” vol. Series A: Applied Mathematics and Physics, 2019.

[18] P. Constantin et al, „Design of the gas cell for the IGISOL facility at ELI-NP,” 2017.

[19] de Hoffmann Edmond et al, Mass Spectrometry: Principles and Applications (Second ed.)., 2003.

[20] D.L. Balabanski et al, „Photo-fission Experiments at ELI-NP,” 2016.

[21] Constantin Paul et al, „The ELI-NP IGISOL radioactive ion beam facility.,” vol. Section B: Beam Interactions with Materials and Atoms, 2019.

[22] P. Constantin et al, 20165.

[23] Dahl D. et al, 2000.

[24] Board, Printed Circuit, „Printed Circuit Board,” [Interactiv]. Available: https://en.wikipedia.org/wiki/Printed_circuit_board.

[25] Eurocircuits, „Eurocircuits PCB materials,” [Interactiv]. Available: https://www.eurocircuits.com.

[26] Wrede, C., „The Facility for Rare Isotope Beams,” 2015.

[27] Geissel, H. et al, „The Super-FRS project at GSI.,” vol. Section B: Beam Interactions with Materials and Atoms, 2003.

[28] B. Harss et al, „Production of radioactive ion beams using the in-flight technique,” 2000.

[29] V. M. Miklyaev et al, Application of Pt1000 C420 Thin-Film Temperature Sensors at Superconducting and Other Types of Facilities, Springer.

[30] Corregidor V. et al, „The External Ion Beam Facility in Portugal for Studying Cultural Heritage,” *e-conservation magazine,* pp. 22. 40-52., 2011.

[31] Lehnert J. et al, „Ion Beam Induced Charge analysis of diamond diodes,” vol. Section B: Beam Interactions with Materials and Atoms, nr. 404. 10.1016/j.nimb.2017.01.021., 2017.